

Dy^{III} single-molecule magnets from ligands incorporating both amine and acylhydrazine Schiff base groups: the centrosymmetric {Dy₂} displaying dual magnetic relaxation behaviors

Sen-Da Su,^a Jia-Xin Li,^b Fan Xu,^a Chen-Xiao Wang,^a Kai Wang,*^a Yan Li,^a Shu-Hua Zhang,^a Xiu-Qing Zhang,^a Yi-Quan Zhang*^b and Fu-Pei Liang*^a

Table of contents:

1. **Figure S1.** IR spectrum of **1-3**, free Hpphz and H₃aahz ligands.
2. **Figure S2.** TG curves of **1-3**.
3. **Figure S3.** The PXRD patterns of **1-3**.
4. **Figure S4.** Molecular structure (a), [Dy₂(OAc)₂] core (b) and coordination geometry of the Dy^{III} ions of **2**.
5. **Table S1.** CShM values calculated by SHAPE for Dy^{III} ions in **1**.
6. **Table S2.** CShM values calculated by SHAPE for Dy^{III} ions in **2**.
7. **Figure S5.** Two discrete {Dy₆} clusters in molecular structure of **3**.
8. **Table S3.** CShM values calculated by SHAPE for Dy^{III} ions in **3**.
9. **Figure S6.** The plots of $M-HT^{-1}$ of **1-3**.
10. **Figure S7.** Frequency-dependent χ' ac susceptibilities of **1-2** under zero and 1.0 kOe fields.
11. **Table S4.** The best fitting parameters of **1** from of ac data under zero applied dc field.

^aGuangxi Key Laboratory of Electrochemical and Magnetochemical Functional Materials, College of Chemistry and Bioengineering, Guilin University of Technology, Guilin, 541004, China.

E-mail: fliangoffice@yahoo.com; kaiwang2011@yahoo.com

^bJiangsu Key Lab for NSLSCS, School of Physical Science and Technology, Nanjing Normal University, Nanjing 210023, China. E-mail: zhangyiquan@njnu.edu.cn

12. **Table S5.** The best fitting parameters of **2** from of ac data under zero applied dc field.
13. **Figure S8.** Frequency-dependent χ'' for **1-2** at 2 K under different dc fields.
14. **Table S6.** The best fitting parameters of **1** from of ac data under 1.0 kOe applied dc field.
15. **Table S7.** The best fitting parameters of **2** from of ac data under 1.0 kOe applied dc field.
16. **Figure S9.** Frequency-dependent χ' ac susceptibilities of **1@Y** and **2@Y** under zero and 0.4 kOe fields.
17. **Table S8.** The best fitting parameters of **1@Y** from of ac data under zero applied dc field.
18. **Table S9.** The best fitting parameters of **2@Y** from of ac data under zero applied dc field.
19. **Figure S10.** Frequency-dependent χ'' for **1-2** at 2 K under different dc fields.
20. **Table S10.** The best fitting parameters of **1@Y** from of ac data under 0.4 kOe applied dc field.
21. **Table S11.** The best fitting parameters of **2@Y** from of ac data under 0.4 kOe applied dc field.
22. **Figure S11.** Frequency-dependent χ' ac susceptibilities of **3** under zero and 2.0 kOe field.
23. **Table S12.** The best fitting parameters of **3** from of ac data under zero applied dc field.
24. **Figure S12.** Frequency-dependent χ'' for **3** at 2 K under different dc fields.
25. **Table S13.** The best fitting parameters of **3** from of ac data under 2.0 kOe applied dc field.
26. **Computational details**
27. **Figure S13.** Calculated model structures of **Dy1** fragments in **1-3**; H atoms are omitted.
28. **Table S14.** Calculated energy levels (cm^{-1}), \mathbf{g} (g_x , g_y , g_z) tensors and predominant m_J values of the lowest eight Kramers doublets (KDs) of individual Dy^{III} fragments for **1-3** using CASSCF/RASSI-SO with MOLCAS 8.4.
29. **Table S15.** Wave functions with definite projection of the total moment $|m_J\rangle$ for the lowest two KDs of individual Dy^{III} fragments for **1-3** using CASSCF/RASSI-SO with MOLCAS 8.4.
30. **Figure S14.** Magnetization blocking barriers for individual Dy^{III} fragments in **1-3**.

31. **Figure S15.** Calculated (red solid line) and experimental (black circle dot) data of magnetic susceptibilities of **1** (left) and **2** (right).
32. **Table S16.** Relevant parameters for the calculation of intermolecular magnetic interactions of **1** and **2**.
33. **Table S17.** Exchange energies E (cm^{-1}), the energy difference between each exchange doublets Δ_t (cm^{-1}) and the main values of the g_z for the lowest two exchange doublets of **1–2**.
34. **Figure S16.** Calculated orientations of the local main magnetic axes on Dy^{III} ions of **1** (left) and **2** (right) in the ground KDs
35. **References**
36. **Scheme S1.** Synthetic route of the Hpphz and H_3sshz ligands.
37. **Figure S17.** ^1H NMR of the Hpphz (top) and H_3sshz (down) ligands.
38. **Table S18.** Dy^{III} and Y^{III} ion contents of **1@Y** and **2@Y** determined by energy dispersive spectroscope (EDS) of field-emission scanning electron microscope.
39. **Table S19.** Crystal data and structure refinement parameters for **1–3**.
40. **Figure S18.** Perspective ORTEP drawing of **1** (the hydrogen atoms were omitted for clarity).
41. **Figure S19.** Perspective ORTEP drawing of **2** (the hydrogen atoms were omitted for clarity).
42. **Figure S20.** Perspective ORTEP drawing of **3** (the hydrogen atoms were omitted for clarity).
43. **Table S20.** Selected bond lengths (\AA) and angles ($^\circ$) for **1**.
44. **Table S21.** Selected bond lengths (\AA) and angles ($^\circ$) for **2**.
45. **Table S22.** Selected bond lengths (\AA) and angles ($^\circ$) for **3**.

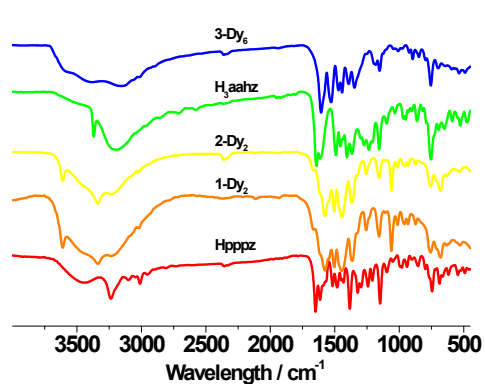


Figure S1. IR spectrum of 1-3, free Hpphz and H₃aahz ligands.

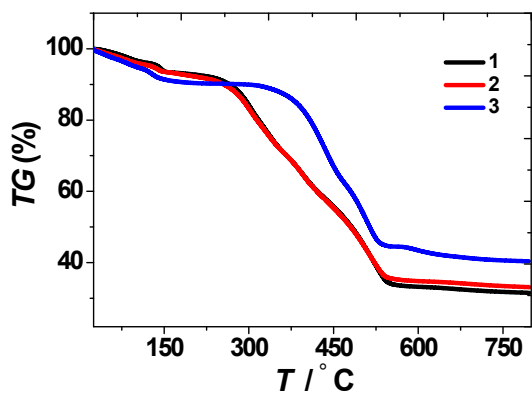


Figure S2. TG curves of 1-3.

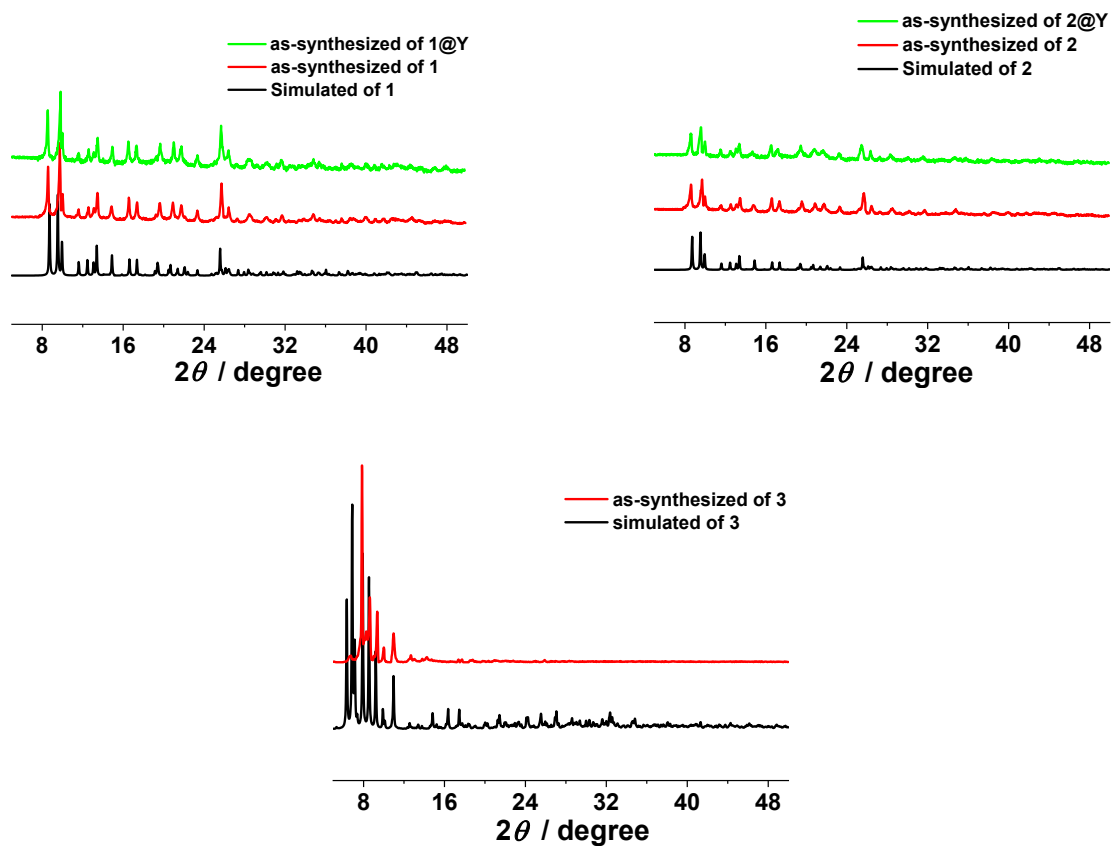


Figure S3. The PXRD patterns of 1-3.

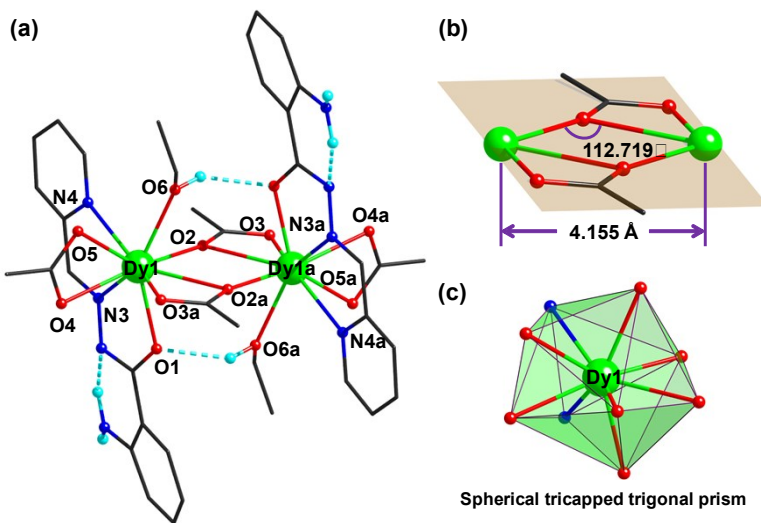


Figure S4. Molecular structure (a), $[\text{Dy}_2(\text{OAc})_2]$ core (b) and coordination geometry of the Dy^{III} ions of **2**.

Table S1. CShM values calculated by SHAPE for Dy^{III} ions in **1**.

Configurations	Symmetry	CShM values
Enneagon	D_{9h}	33.472
Octagonal pyramid	C_{8v}	23.540
Heptagonal bipyramid	D_{7h}	18.131
Johnson triangular cupola J3	C_{3v}	12.651
Capped cube J8	C_{4v}	9.347
Spherical-relaxed capped cube	C_{4v}	8.697
Capped square antiprism J10	C_{4v}	2.660
Spherical capped square antiprism	C_{4v}	2.288
Tricapped trigonal prism J51	D_{3h}	2.891
Spherical tricapped trigonal prism	D_{3h}	2.308
Tridiminished icosahedron J63	C_{3v}	11.248

Table S2. CShM values calculated by SHAPE for Dy^{III} ions in **2**.

Configurations	Symmetry	CShM values
Enneagon	D_{9h}	33.391
Octagonal pyramid	C_{8v}	23.328
Heptagonal bipyramid	D_{7h}	17.990
Johnson triangular cupola J3	C_{3v}	12.637
Capped cube J8	C_{4v}	9.345
Spherical-relaxed capped cube	C_{4v}	8.636
Capped square antiprism J10	C_{4v}	2.736
Spherical capped square	C_{4v}	2.400
Tricapped trigonal prism J51	D_{3h}	2.905
Spherical tricapped trigonal	D_{3h}	2.359
Tridiminished icosahedron J63	C_{3v}	11.281

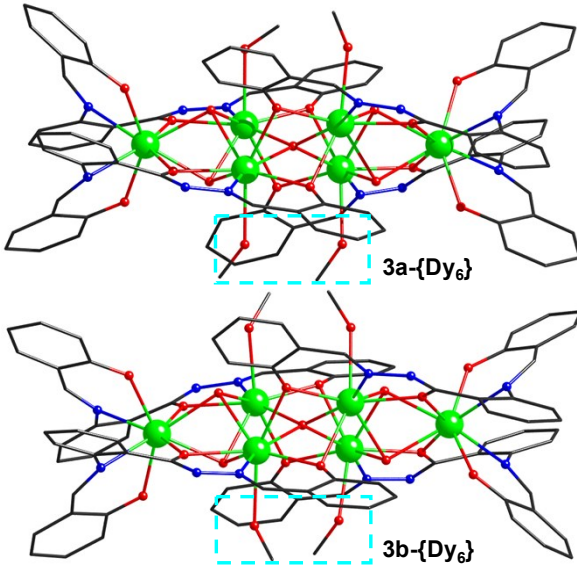


Figure S5. Two discrete $\{\text{Dy}_6\}$ clusters in molecular structure of **3**.

Table S3. CShM values calculated by SHAPE for Dy^{III} ions in **3**.

Configurations	Symmetry	CShM values					
		Dy1	Dy2	Dy3	Dy4	Dy5	Dy6
Octagon	$D_{8\text{h}}$	26.874	27.224	26.894	28.065	31.582	30.286
Heptagonal pyramid	$C_{7\text{v}}$	23.012	22.666	23.46	22.326	22.649	21.111
Hexagonal bipyramid	$D_{6\text{h}}$	15.748	15.74	14.622	15.522	16.636	16.107
Cube	O_{h}	12.15	12.343	12.219	12.7	9.839	10.005
Square antiprism	$D_{4\text{d}}$	1.481	1.829	1.821	2.421	2.241	1.392
Triangular dodecahedron	$D_{2\text{d}}$	1.887	1.616	2.054	1.772	0.991	1.793
Johnson gyrobifastigium J26	$D_{2\text{d}}$	13.774	13.2	12.15	12.562	12.747	14.133
Johnson elongated triangular bipyramid J14	$D_{3\text{h}}$	26.586	26.328	25.367	25.994	28.775	27.68
Biaugmented trigonal prism J50	$C_{2\text{v}}$	2.445	2.59	3.015	2.994	2.855	2.539
Biaugmented trigonal prism	$C_{2\text{v}}$	1.601	1.758	2.178	2.137	2.555	2.247
Snub diphenoïd J84	$D_{2\text{d}}$	3.949	3.47	3.851	3.585	2.841	3.7
Configurations	Symmetry	CShM values					
		Dy7	Dy8	Dy9	Dy10	Dy11	Dy12
Octagon	$D_{8\text{h}}$	26.891	27.333	28.836	27.938	30.979	30.288
Heptagonal pyramid	$C_{7\text{v}}$	23.215	22.164	20.589	23.42	22.1	20.539
Hexagonal bipyramid	$D_{6\text{h}}$	15.082	14.844	16.151	15.233	16.087	15.783
Cube	O_{h}	12.407	13.025	13.772	12.493	9.525	9.968
Square antiprism	$D_{4\text{d}}$	1.701	2.586	3.735	1.953	2.044	1.422
Triangular dodecahedron	$D_{2\text{d}}$	1.987	2.273	2.391	1.539	0.992	2.201
Johnson gyrobifastigium J26	$D_{2\text{d}}$	12.848	11.804	12.526	12.745	13.313	14.681
Johnson elongated triangular bipyramid J14	$D_{3\text{h}}$	26.302	25.962	26.203	26.961	28.843	27.458
Biaugmented trigonal prism J50	$C_{2\text{v}}$	2.746	2.915	3.164	2.85	2.618	2.713
Biaugmented trigonal prism	$C_{2\text{v}}$	1.839	1.936	2.237	2.091	2.49	2.462
Snub diphenoïd J84	$D_{2\text{d}}$	3.957	3.953	4.02	3.403	2.875	4.165

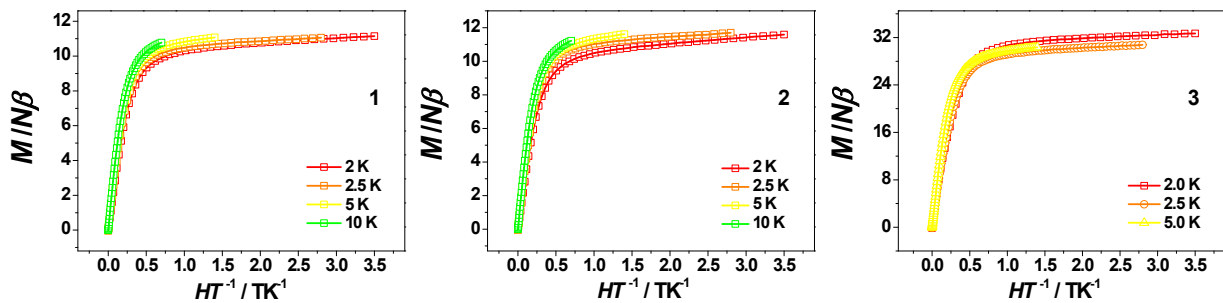


Figure S6. The plots of $M-HT^{-1}$ of **1-3**.

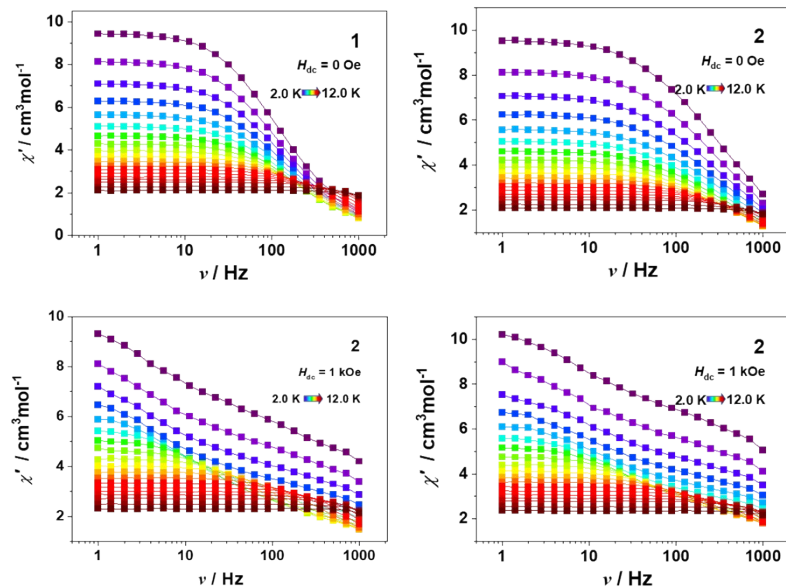


Figure S7. Frequency-dependent χ' ac susceptibilities of **1-2** under zero and 1.0 kOe fields.

Table S4. The best fitting parameters of **1** from of ac data under zero applied dc field.

T (K)	χ_s	χ_T	τ	a
2	0.494447E+00	0.959224E+01	0.133495E-02	0.214583E+00
2.5	0.428643E+00	0.824745E+01	0.126730E-02	0.218789E+00
3	0.398085E+00	0.719547E+01	0.118278E-02	0.220279E+00
3.5	0.373139E+00	0.637404E+01	0.110410E-02	0.221546E+00
4	0.346463E+00	0.571764E+01	0.102639E-02	0.221326E+00
4.5	0.342031E+00	0.516694E+01	0.966060E-03	0.215002E+00
5	0.324618E+00	0.470549E+01	0.880135E-03	0.205986E+00
5.5	0.316557E+00	0.431840E+01	0.783240E-03	0.190930E+00

6	0.302965E+00	0.399108E+01	0.671178E-03	0.174686E+00
6.5	0.286409E+00	0.371291E+01	0.556301E-03	0.161823E+00
7	0.281181E+00	0.347131E+01	0.450536E-03	0.152044E+00
7.5	0.302509E+00	0.326233E+01	0.359714E-03	0.141671E+00
8	0.343508E+00	0.308088E+01	0.287018E-03	0.135553E+00
8.5	0.417056E+00	0.291646E+01	0.230694E-03	0.130733E+00
9	0.540733E+00	0.275478E+01	0.189119E-03	0.116189E+00
9.5	0.705683E+00	0.261941E+01	0.159808E-03	0.102746E+00
10	0.900886E+00	0.250158E+01	0.140594E-03	0.902648E-01
11	0.134920E+01	0.228476E+01	0.133976E-03	0.283391E-01
12	0.156998E+01	0.210311E+01	0.127788E-03	0.168191E-18
13	0.167412E+01	0.195287E+01	0.134354E-03	0.333965E-18
14	0.168199E+01	0.182010E+01	0.155104E-03	0.481121E-18

Table S5. The best fitting parameters of **2** from of ac data under zero applied dc field.

T/K	χ_s	χ_T	τ	a
2	8.626210E-01	9.666910E+00	5.934760E-04	2.959790E-01
2.5	7.486330E-01	8.245470E+00	5.919860E-04	2.977950E-01
3	7.037080E-01	7.173070E+00	5.955190E-04	2.998580E-01
3.5	6.552810E-01	6.338260E+00	5.848020E-04	3.007360E-01
4	6.188970E-01	5.660470E+00	5.780630E-04	3.007140E-01
4.5	6.166480E-01	5.116790E+00	5.712070E-04	2.920900E-01
5	6.050310E-01	4.667890E+00	5.560920E-04	2.823410E-01
5.5	6.093090E-01	4.282510E+00	5.326560E-04	2.646150E-01
6	5.872420E-01	3.971390E+00	4.891410E-04	2.505610E-01
6.5	6.021730E-01	3.685290E+00	4.503960E-04	2.262360E-01
7	5.878480E-01	3.448470E+00	3.855740E-04	2.073750E-01
7.5	5.928920E-01	3.223790E+00	3.315320E-04	1.928000E-01
8	6.163490E-01	3.041230E+00	2.750110E-04	1.820190E-01
8.5	6.834030E-01	2.882720E+00	2.261240E-04	1.746770E-01
9	8.241300E-01	2.719440E+00	1.899940E-04	1.620320E-01
9.5	1.045050E+00	2.586770E+00	1.731920E-04	1.468420E-01
10	1.301570E+00	2.470070E+00	1.754110E-04	1.084530E-01
11	1.577570E+00	2.250890E+00	1.751670E-04	3.605880E-02
12	1.674610E+00	2.082930E+00	1.609400E-04	4.263250E-14
13	1.698470E+00	1.930420E+00	1.619120E-04	7.854740E-14
14	1.673390E+00	1.801200E+00	1.802710E-04	8.473630E-14
15	1.619810E+00	1.696700E+00	2.023640E-04	1.580340E-13

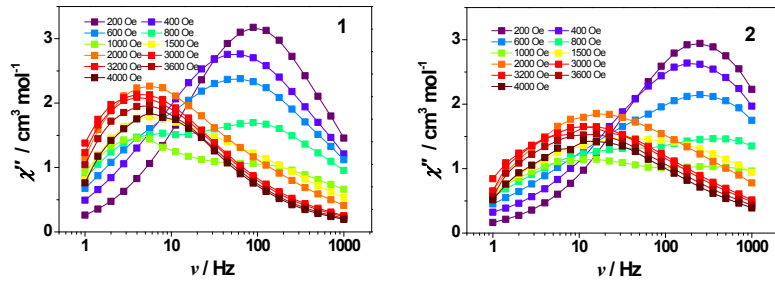


Figure S8. Frequency-dependent χ'' for **1-2** at 2 K under different dc fields.

Table S6. The best fitting parameters of **1** from of ac data under 1 kOe applied dc field.

T/K	χ_s	$\Delta\chi_1$	τ_1	α_1	$\Delta\chi_2$	τ_2	α_2
2	3.751180E+00	2.717980E+00	6.880650E-04	3.122580E-01	3.845570E+00	4.680360E-02	3.078710E-01
2.5	2.859930E+00	2.383470E+00	5.085910E-04	3.300190E-01	3.736720E+00	4.731150E-02	2.931920E-01
3	2.336490E+00	2.023190E+00	4.228570E-04	3.295630E-01	3.545660E+00	4.068540E-02	2.784630E-01
3.5	1.901890E+00	2.052100E+00	4.358510E-04	3.878840E-01	2.951470E+00	3.271000E-02	2.137090E-01
4	1.726630E+00	1.637940E+00	3.917000E-04	3.400730E-01	2.833560E+00	2.206600E-02	1.970510E-01
4.5	1.626540E+00	1.228950E+00	3.471390E-04	2.564080E-01	2.725780E+00	1.286830E-02	1.769430E-01
5	1.448780E+00	1.236700E+00	3.826150E-04	2.910020E-01	2.405070E+00	7.967230E-03	1.317160E-01
5.5	1.410180E+00	7.893790E-01	2.986160E-04	1.455690E-01	2.482000E+00	4.236820E-03	1.386050E-01
6	1.310230E+00	8.608070E-01	3.430240E-04	1.506920E-01	2.140130E+00	2.628970E-03	1.025540E-01
6.5	1.277690E+00	6.031130E-01	2.769650E-04	2.067100E-05	2.142290E+00	1.553740E-03	1.053870E-01
7	1.216490E+00	7.422730E-01	2.623090E-04	1.187580E-05	1.820020E+00	1.074220E-03	9.046890E-02
7.5	1.195760E+00	9.501780E-01	2.462770E-04	2.126910E-05	1.394880E+00	8.054730E-04	8.120130E-02
8	1.226130E+00	1.166090E+00	2.215850E-04	3.840760E-05	9.475620E-01	6.454420E-04	7.577200E-02
8.5	1.298360E+00	1.347590E+00	1.954470E-04	4.969400E-05	5.071890E-01	6.050220E-04	6.029330E-02
9	1.427700E+00	1.386930E+00	1.759370E-04	3.321930E-04	1.815830E-01	7.301520E-04	3.738450E-06
9.5	1.580340E+00	1.208410E+00	1.552640E-04	3.025510E-04	7.205610E-02	8.708840E-04	1.047830E-05
10	1.738400E+00	9.605020E-01	1.441950E-04	4.930990E-04	1.502220E-02	9.687740E-04	2.156150E-05
11	1.963750E+00	5.224490E-01	1.314670E-04	1.171800E-03	3.731100E-08	1.859330E-03	2.984380E-05
12	2.049040E+00	2.519550E-01	1.395290E-04	1.210410E-09	1.267570E-07	5.006080E-03	1.123060E-04
13	2.007290E+00	1.182610E-01	1.769800E-04	1.565030E-09	1.343610E-07	5.585670E-03	1.173890E-04
14	1.915450E+00	6.790250E-02	2.188370E-04	1.851890E-09	1.568800E-07	6.897780E-03	1.752810E-04
15	1.809130E+00	4.856800E-02	2.479700E-04	3.112080E-09	1.367360E-07	9.229780E-03	5.461550E-05
16	1.716540E+00	3.865850E-02	2.785020E-04	3.069600E-09	1.618510E-07	1.090890E-02	5.936530E-05
17	1.621970E+00	3.322470E-02	2.942330E-04	4.479200E-09	1.749170E-07	1.197530E-02	6.615960E-05

Table S7. The best fitting parameters of **2** from of ac data under 1 kOe applied dc field.

T/K	χ_s	$\Delta\chi_1$	τ_1	α_1	$\Delta\chi_2$	τ_2	α_2
2	3.897500E+00	3.451510E+00	2.915440E-04	3.681180E-01	3.208560E+00	2.150940E-02	2.475630E-01
2.5	3.382980E+00	2.249520E+00	2.750440E-04	2.721500E-01	3.443250E+00	1.988040E-02	3.102410E-01
3	3.052850E+00	1.119780E+00	2.321090E-04	6.783390E-02	3.899310E+00	1.442660E-02	3.935850E-01
3.5	2.513620E+00	1.587930E+00	2.662070E-04	2.735980E-01	2.960970E+00	1.593920E-02	2.826660E-01

4	2.276370E+00	1.345430E+00	2.753640E-04	2.576940E-01	2.711460E+00	1.276280E-02	2.500320E-01
4.5	2.124630E+00	1.036710E+00	2.668790E-04	1.955990E-01	2.576100E+00	9.127730E-03	2.300070E-01
5	1.937360E+00	1.012610E+00	2.895890E-04	2.185850E-01	2.268440E+00	6.648210E-03	1.755740E-01
5.5	1.851200E+00	7.634230E-01	2.787760E-04	1.321030E-01	2.184200E+00	4.255160E-03	1.618440E-01
6	1.764410E+00	5.706220E-01	2.559660E-04	3.287800E-02	2.096370E+00	2.661990E-03	1.442520E-01
6.5	1.656970E+00	5.747680E-01	2.619200E-04	5.321450E-02	1.897220E+00	1.763200E-03	1.295800E-01
7	1.597100E+00	5.630350E-01	2.641340E-04	1.984120E-12	1.698940E+00	1.213920E-03	1.152420E-01
7.5	1.545600E+00	7.041370E-01	2.670910E-04	2.818940E-12	1.387970E+00	8.831090E-04	1.159130E-01
8	1.524670E+00	1.076200E+00	2.489950E-04	6.319800E-12	8.234050E-01	8.392220E-04	9.614380E-02
8.5	1.545800E+00	1.306790E+00	2.117250E-04	1.235980E-11	3.768040E-01	9.930030E-04	3.445780E-02
9	1.636470E+00	1.145270E+00	1.688510E-04	1.023700E-15	2.867040E-01	8.199250E-04	6.722890E-02
9.5	1.826080E+00	9.450240E-01	1.590890E-04	1.278580E-15	1.455690E-01	8.462710E-04	9.833970E-04
10	2.003690E+00	7.357440E-01	1.709990E-04	1.638240E-15	4.571310E-02	9.530550E-04	1.714530E-03
11	2.124700E+00	4.172490E-01	1.717770E-04	2.195030E-15	1.535940E-14	1.815090E-03	2.801960E-03
12	2.133460E+00	2.209990E-01	1.644600E-04	3.174780E-15	2.248870E-15	2.858570E-03	3.329090E-03
13	2.064170E+00	1.099220E-01	1.878340E-04	3.755910E-15	2.593420E-15	3.411890E-03	3.865950E-03
14	1.966220E+00	6.038960E-02	2.276510E-04	4.248390E-15	1.430710E-15	4.019020E-03	3.209670E-03
15	1.858810E+00	4.268140E-02	2.630610E-04	5.327200E-15	1.768600E-15	4.290830E-03	3.729970E-03

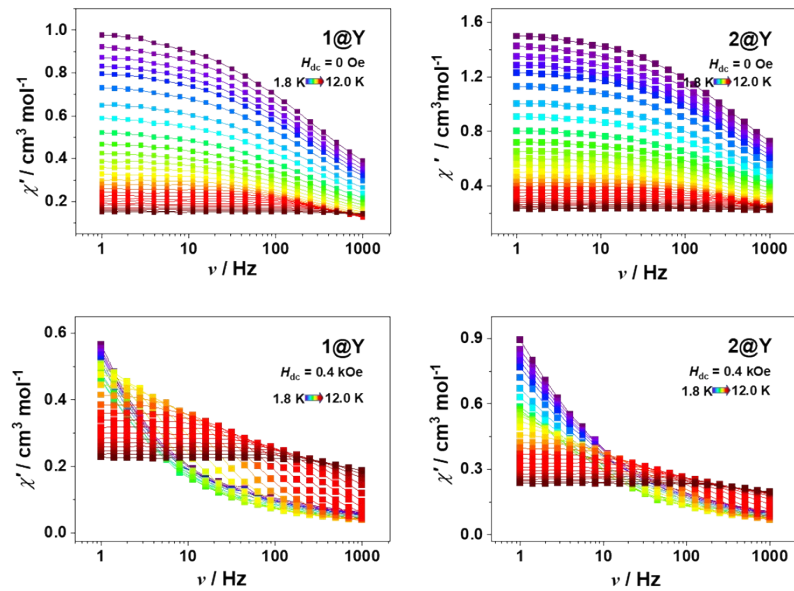


Figure S9. Frequency-dependent χ' ac susceptibilities of **1@Y** and **2@Y** under zero and 1.0 kOe fields.

Table S8. The best fitting parameters of **1@Y** from of ac data under zero applied dc field.

T/K	χ_s	χ_T	τ	a
1.8	6.443900E-02	1.011550E+00	4.954670E-04	4.905730E-01
1.9	6.729010E-02	9.537950E-01	4.965020E-04	4.828670E-01
2	6.822390E-02	9.040670E-01	5.027040E-04	4.803680E-01
2.1	6.315050E-02	8.618260E-01	4.980060E-04	4.800290E-01
2.2	6.111400E-02	8.244350E-01	5.005770E-04	4.811900E-01
2.4	5.367420E-02	7.581770E-01	4.927160E-04	4.831160E-01
2.7	5.168760E-02	6.753500E-01	4.957240E-04	4.807540E-01
3	4.431250E-02	6.089300E-01	4.791410E-04	4.843120E-01
3.4	4.071720E-02	5.393450E-01	4.650190E-04	4.860370E-01
3.8	4.659740E-02	4.831970E-01	4.745030E-04	4.764790E-01
4.2	4.824300E-02	4.376640E-01	4.660330E-04	4.681020E-01
4.6	5.416370E-02	4.003440E-01	4.781120E-04	4.518920E-01
5	6.151850E-02	3.679150E-01	4.922740E-04	4.280820E-01
5.5	6.653070E-02	3.335340E-01	4.846710E-04	3.927990E-01
6	7.151780E-02	3.057200E-01	4.760640E-04	3.491770E-01
6.5	7.212700E-02	2.834890E-01	4.420770E-04	3.151320E-01
7	7.260870E-02	2.616430E-01	3.917460E-04	2.702310E-01
7.5	6.691720E-02	2.441730E-01	3.197680E-04	2.451410E-01
8	6.721020E-02	2.279540E-01	2.731920E-04	2.060730E-01
8.5	6.449740E-02	2.135960E-01	2.220340E-04	1.760580E-01
9	5.734960E-02	2.028640E-01	1.705570E-04	1.774340E-01
9.5	5.644700E-02	1.911410E-01	1.377090E-04	1.538750E-01
10	4.360510E-02	1.821560E-01	9.498290E-05	1.686680E-01
10.5	4.936760E-02	1.728280E-01	8.127170E-05	1.336740E-01
11	4.276890E-02	1.651700E-01	5.861800E-05	1.344970E-01
11.5	1.477770E-02	1.578560E-01	3.316750E-05	1.374580E-01
12	4.195590E-14	1.516640E-01	2.195280E-05	1.462270E-01

Table S9. The best fitting parameters of **2@Y** from of ac data under zero applied dc field.

T/K	χ_s	χ_T	τ	a
1.8	1.755770E-01	1.534990E+00	3.015890E-04	4.653050E-01
1.9	1.574660E-01	1.455630E+00	2.939570E-04	4.689380E-01
2	1.602240E-01	1.382150E+00	2.997300E-04	4.651530E-01
2.1	1.534980E-01	1.319050E+00	3.012790E-04	4.670060E-01
2.2	1.413110E-01	1.259980E+00	2.914810E-04	4.670100E-01
2.4	1.490010E-01	1.156560E+00	3.025910E-04	4.616920E-01
2.7	1.246490E-01	1.032100E+00	2.854410E-04	4.705120E-01
3	1.334120E-01	9.283940E-01	2.914270E-04	4.609080E-01
3.4	1.128940E-01	8.225370E-01	2.635380E-04	4.700440E-01

3.8	1.257970E-01	7.363980E-01	2.742090E-04	4.592170E-01
4.2	1.228420E-01	6.670950E-01	2.638900E-04	4.526340E-01
4.6	1.219810E-01	6.125460E-01	2.610430E-04	4.478430E-01
5	1.303380E-01	5.632500E-01	2.727660E-04	4.260210E-01
5.5	1.406550E-01	5.112890E-01	2.828080E-04	3.930080E-01
6	1.422560E-01	4.665410E-01	2.702410E-04	3.547170E-01
6.5	1.435570E-01	4.307060E-01	2.584510E-04	3.140830E-01
7	1.354360E-01	4.003360E-01	2.186860E-04	2.918760E-01
7.5	1.319670E-01	3.726820E-01	1.856590E-04	2.643080E-01
8	1.245540E-01	3.498080E-01	1.468720E-04	2.545730E-01
8.5	1.089660E-01	3.292150E-01	1.058470E-04	2.481200E-01
9	8.657610E-02	3.114090E-01	6.799820E-05	2.632050E-01
9.5	9.734550E-02	2.948380E-01	5.654820E-05	2.518200E-01
10	5.756490E-02	2.800960E-01	2.936980E-05	2.701910E-01
10.5	8.887120E-02	2.676680E-01	2.900960E-05	2.673950E-01
11	5.687100E-02	2.550380E-01	1.648570E-05	2.726550E-01
11.5	3.638660E-07	2.439080E-01	9.152030E-06	2.764000E-01
12	5.698000E-07	2.343030E-01	7.051010E-06	2.616620E-01

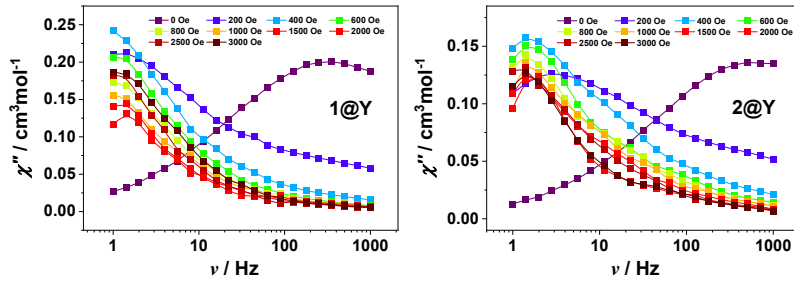


Figure S10. Frequency-dependent χ'' for **1-2** at 2 K under different dc fields.

Table S10. The best fitting parameters of **1@Y** from of ac data under 0.4 kOe applied dc field.

T/K	χ_s	χ_T	τ	a
1.8	5.836460E-02	2.016190E+00	7.795790E-01	4.437910E-01
2	5.269110E-02	1.917700E+00	8.119650E-01	4.598550E-01
2.2	4.899730E-02	1.684600E+00	6.632660E-01	4.609830E-01
2.4	4.748040E-02	1.443300E+00	4.880770E-01	4.545220E-01
2.7	4.223810E-02	1.301940E+00	4.276620E-01	4.586050E-01
3	4.108580E-02	1.185660E+00	3.733050E-01	4.547990E-01
3.4	4.082110E-02	9.975490E-01	2.373250E-01	4.292180E-01
3.8	3.979640E-02	8.581850E-01	1.414460E-01	3.927920E-01
4.2	4.108140E-02	7.316470E-01	7.695370E-02	3.438660E-01
4.6	4.123260E-02	6.283580E-01	4.151550E-02	2.834770E-01

5	3.992660E-02	5.655570E-01	2.470740E-02	2.478110E-01
5.5	3.661900E-02	5.045520E-01	1.331330E-02	2.192750E-01
6	3.274810E-02	4.606250E-01	7.499270E-03	1.962370E-01
6.5	3.023760E-02	4.237670E-01	4.447480E-03	1.907580E-01
7	2.827310E-02	3.914320E-01	2.720660E-03	1.786890E-01
7.5	2.676490E-02	3.648200E-01	1.725480E-03	1.670570E-01
8	2.574780E-02	3.416690E-01	1.122250E-03	1.666510E-01
8.5	2.676360E-02	3.215620E-01	7.545900E-04	1.622590E-01
9	2.908170E-02	3.027540E-01	5.193010E-04	1.621280E-01
9.5	2.766910E-02	2.870200E-01	3.558980E-04	1.657680E-01
10	3.668890E-02	2.729460E-01	2.591220E-04	1.586110E-01
10.5	3.922800E-02	2.606320E-01	1.820380E-04	1.700540E-01
11	4.878160E-02	2.484230E-01	1.330470E-04	1.709200E-01
11.5	6.353950E-02	2.375170E-01	1.062500E-04	1.532590E-01
12	6.174810E-02	2.270390E-01	7.036310E-05	1.726310E-01

Table S11. The best fitting parameters of **2@Y** from of ac data under 0.4 kOe applied dc field.

T/K	χ_s	χ_T	τ	a
1.8	7.933020E-02	1.846370E+00	2.192960E-01	4.995500E-01
1.9	6.562900E-02	1.918090E+00	2.941950E-01	5.365090E-01
2	6.424060E-02	1.748710E+00	2.348140E-01	5.291690E-01
2.1	6.342640E-02	1.623540E+00	2.004530E-01	5.206980E-01
2.2	6.529080E-02	1.534390E+00	1.876910E-01	5.204020E-01
2.4	6.102760E-02	1.400550E+00	1.687670E-01	5.258170E-01
2.7	5.984560E-02	1.294140E+00	1.734280E-01	5.290410E-01
3	6.239580E-02	1.137280E+00	1.360000E-01	5.117120E-01
3.4	5.765610E-02	9.953220E-01	1.006890E-01	5.087620E-01
3.8	6.198340E-02	8.415070E-01	6.250430E-02	4.597120E-01
4.2	6.272120E-02	7.313330E-01	3.790100E-02	4.137450E-01
4.6	6.461670E-02	6.571600E-01	2.574450E-02	3.796320E-01
5	6.198870E-02	5.834980E-01	1.521780E-02	3.399220E-01
5.5	5.949270E-02	5.266520E-01	8.953980E-03	3.096750E-01
6	5.430810E-02	4.768870E-01	5.293190E-03	2.880950E-01
6.5	5.130200E-02	4.377200E-01	3.201900E-03	2.672590E-01
7	5.023220E-02	4.071050E-01	2.022520E-03	2.605740E-01
7.5	4.549980E-02	3.753470E-01	1.245190E-03	2.651560E-01
8	4.626280E-02	3.547090E-01	8.335240E-04	2.743660E-01
8.5	5.331770E-02	3.341950E-01	5.563630E-04	2.711240E-01
9	5.507770E-02	3.152080E-01	3.590840E-04	3.031950E-01

9.5	7.659340E-02	2.983460E-01	2.837710E-04	2.952770E-01
10	1.034230E-01	2.826470E-01	2.535340E-04	2.729650E-01
10.5	1.228290E-01	2.682680E-01	2.333420E-04	2.375000E-01
11	1.237970E-01	2.560150E-01	1.803870E-04	2.496780E-01
11.5	1.438500E-01	2.442580E-01	1.805800E-04	1.834290E-01
12	1.584950E-01	2.368610E-01	1.850260E-04	1.373110E-01

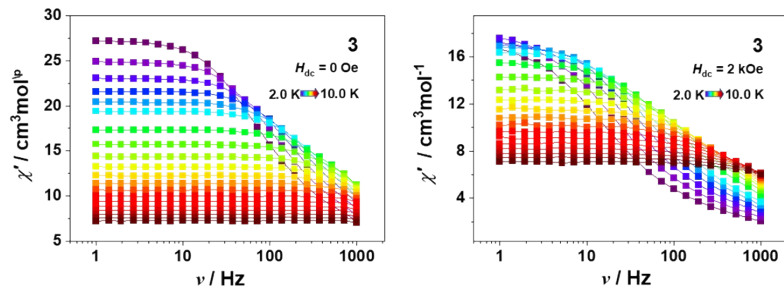


Figure S11. Frequency-dependent χ' ac susceptibilities of **3** under zero and 2.0 kOe field.

Table S12. The best fitting parameters of **3** from of ac data under zero applied dc field.

T/K	χ_s	χ_T	τ	a
2	5.927760E+00	2.780550E+01	1.838700E-03	2.286730E-01
2.2	6.035680E+00	2.527400E+01	1.123980E-03	2.137980E-01
2.4	6.200360E+00	2.333770E+01	7.502040E-04	2.011190E-01
2.6	6.373940E+00	2.181910E+01	5.400960E-04	1.903960E-01
2.8	6.543520E+00	2.056920E+01	4.117000E-04	1.812750E-01
3	6.722260E+00	1.951100E+01	3.305390E-04	1.709220E-01
3.5	7.099990E+00	1.738950E+01	2.230470E-04	1.456040E-01
4	7.311820E+00	1.574860E+01	1.739250E-04	1.220570E-01
4.5	7.390820E+00	1.439250E+01	1.475340E-04	9.719980E-02
5	7.391680E+00	1.324270E+01	1.296910E-04	7.388460E-02
5.5	7.365270E+00	1.225860E+01	1.161260E-04	5.243720E-02
6	7.453220E+00	1.140230E+01	1.079260E-04	2.509400E-02
6.5	7.520100E+00	1.065390E+01	1.013290E-04	6.404190E-15
7	7.424060E+00	9.993650E+00	8.906530E-05	2.866490E-16
7.5	7.396010E+00	9.403120E+00	8.183100E-05	4.404310E-16
8	7.386890E+00	8.879560E+00	7.903160E-05	6.625540E-16
8.5	7.356360E+00	8.407240E+00	7.976720E-05	9.851760E-16
9	7.271250E+00	7.982630E+00	8.389270E-05	1.563450E-15
9.5	7.161680E+00	7.594930E+00	9.594450E-05	1.905500E-15
10	6.987120E+00	7.243450E+00	1.119280E-04	3.652630E-15

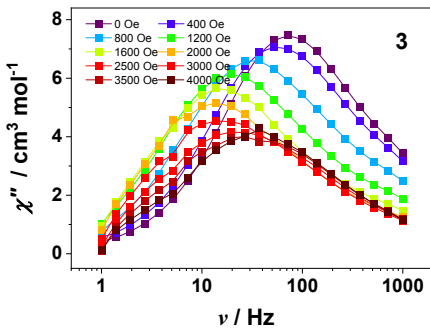


Figure S12. Frequency-dependent χ'' for **3** at 2 K under different dc fields.

Table S13. The best fitting parameters of **3** from ac data under 2.0 kOe applied dc field.

T/K	χ_s	χ_T	τ	a
2	1.662970E+00	1.800630E+01	8.715460E-03	3.236350E-01
2.2	1.837210E+00	1.838600E+01	6.168570E-03	3.246560E-01
2.4	2.037190E+00	1.812290E+01	4.286980E-03	3.141620E-01
2.6	2.255640E+00	1.775480E+01	3.159330E-03	3.017300E-01
2.8	2.372850E+00	1.746570E+01	2.460080E-03	2.998690E-01
3	2.466300E+00	1.688370E+01	1.916210E-03	2.948800E-01
3.5	2.621800E+00	1.574230E+01	1.198520E-03	2.884860E-01
4	2.737560E+00	1.453150E+01	8.298990E-04	2.765520E-01
4.5	2.805880E+00	1.341140E+01	6.125660E-04	2.639340E-01
5	2.823710E+00	1.248940E+01	4.764840E-04	2.567560E-01
5.5	2.807170E+00	1.166240E+01	3.740260E-04	2.537460E-01
6	2.919340E+00	1.090800E+01	3.054770E-04	2.420010E-01
6.5	2.851920E+00	1.027100E+01	2.417980E-04	2.503340E-01
7	2.932250E+00	9.690580E+00	1.989350E-04	2.495760E-01
7.5	3.139140E+00	9.151430E+00	1.700320E-04	2.436380E-01
8	3.303710E+00	8.681750E+00	1.449060E-04	2.473580E-01
8.5	3.517570E+00	8.244550E+00	1.273280E-04	2.474610E-01
9	3.667940E+00	7.840900E+00	1.092540E-04	2.564390E-01
9.5	3.988620E+00	7.480200E+00	1.044040E-04	2.533250E-01
10	4.455860E+00	7.111280E+00	1.164700E-04	2.144040E-01

Computational details

Binuclear complexes **1** and **2** both have one type of magnetic center Dy^{III} ion, thus we only need to calculate one Dy^{III} fragment for each of them. Complex **3** has two types of structures indicated as **3a** and **3b** which both have six types of individual Dy^{III} fragments. All of individual Dy^{III} fragments (see Figure S1 for the calculated model structures of **Dy1** fragments in complexes **1–3**) on the basis of single-crystal X-ray determined geometry have been carried out by complete-active-space self-consistent field (CASSCF) with MOLCAS 8.4 program package.^{S1} Each individual Dy^{III} fragment in **1–3** was calculated keeping the experimentally determined structure of the corresponding compound while replacing the other Dy^{III} ions with diamagnetic Lu^{III}.^{S2}

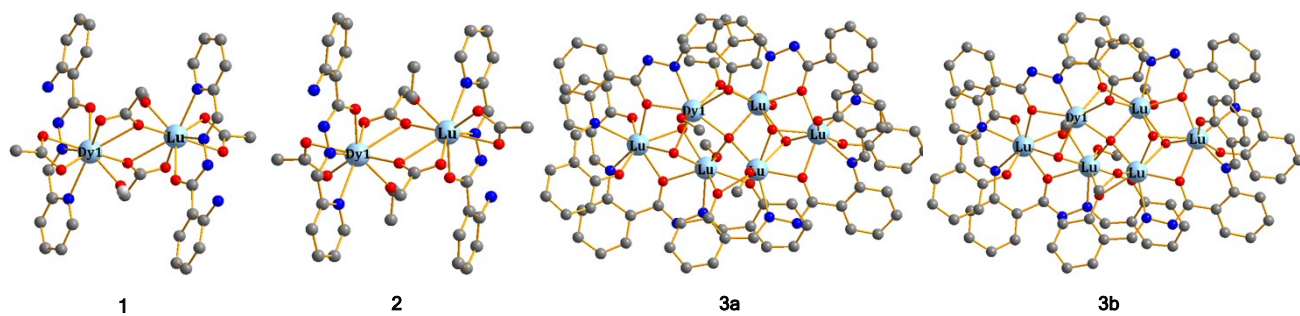


Figure S13. Calculated model structures of **Dy1** fragments in **1–3**; H atoms are omitted.

The basis sets for all atoms are atomic natural orbitals from the MOLCAS ANO-RCC library: ANO-RCC-VTZP for Dy^{III}; VTZ for close O and N; VDZ for distant atoms. The calculations employed the second order Douglas-Kroll-Hess Hamiltonian, where scalar relativistic contractions were taken into account in the basis set and the spin-orbit couplings were handled separately in the restricted active space state interaction (RASSI-SO) procedure. For individual Dy^{III} fragment, active electrons in 7 active spaces include all *f* electrons (CAS(9 in 7 for Dy^{III}) in the CASSCF calculation. To exclude all the doubts, we calculated all the roots in the active space. We have mixed the maximum number of spin-free state which was possible with our hardware (all from 21 sextets, 128 from 224 quadruplets, 130 from 490 doublets for Dy^{III}). SINGLE_ANISO^{S3} program was used to obtain the energy levels, **g** tensors, predominant m_J values, magnetic axes, *et al.*, based on the above CASSCF/RASSI-SO calculations.

Table S14. Calculated energy levels (cm^{-1}), **g** (g_x , g_y , g_z) tensors and predominant m_J values of the lowest eight

Kramers doublets (KDs) of individual Dy^{III} fragments for **1–3** using CASSCF/RASSI-SO with MOLCAS 8.4.

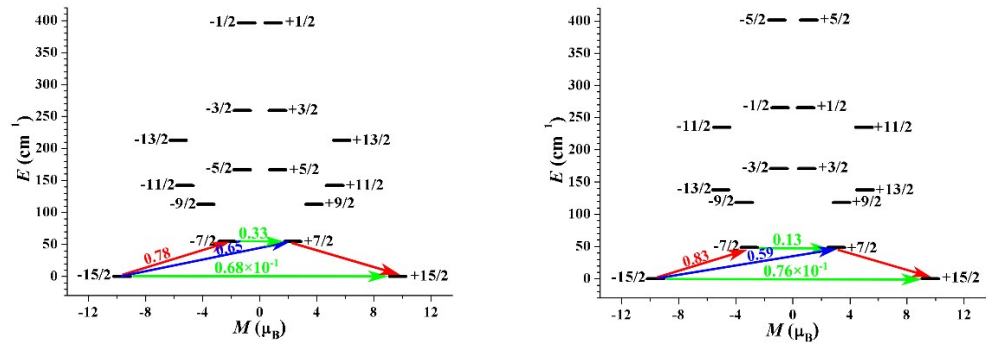
KDs	1_Dy1			2_Dy1			3a_Dy1		
	E/cm ⁻¹	<i>g</i>	<i>m_J</i>	E/cm ⁻¹	<i>g</i>	<i>m_J</i>	E/cm ⁻¹	<i>g</i>	<i>m_J</i>
1	0.0	0.093		0.0	0.091		0.0	0.022	
		0.317	±15/2		0.368	±15/2		0.055	±15/2
		19.318			19.255			19.447	
2	54.5	0.348		48.3	0.090		33.8	0.0151	
		0.490	±7/2		0.321	±7/2		0.0791	±11/2
		18.779			18.919			19.1415	
3	112.8	1.617		118.4	1.339		153.1	1.736	
		1.859	±9/2		2.462	±9/2		2.713	±5/2
		15.615			15.177			15.420	
4	142.1	11.570		137.9	11.258		197.6	5.075	
		6.981	±11/2		6.527	±13/2		6.130	±9/2
		2.314			1.606			7.8153	
5	166.8	0.109		171.0	1.402		257.4	0.708	
		1.297	±5/2		2.379	±3/2		2.666	±3/2
		12.367			12.286			11.766	
6	212.8	0.876		235.2	0.328		338.6	0.784	
		1.068	±13/2		1.057	±11/2		1.389	±1/2
		18.023			18.063			14.980	
7	259.2	0.433		265.5	0.553		427.4	0.298	
		0.729	±3/2		1.230	±1/2		0.393	±7/2
		16.474			15.774			18.581	
8	396.2	0.050		401.2	0.057		706.1	0.007	
		0.062	±1/2		0.068	±5/2		0.011	±13/2
		19.213			19.160			19.757	
KDs	3a_Dy2			3a_Dy3			3a_Dy4		
	E/cm ⁻¹	<i>g</i>	<i>m_J</i>	E/cm ⁻¹	<i>g</i>	<i>m_J</i>	E/cm ⁻¹	<i>g</i>	<i>m_J</i>
1	0.0	0.021		0.0	0.164		0.0	0.009	
		0.039	±15/2		0.602	±15/2		0.015	±15/2
		19.775			18.693			19.785	
2	110.0	0.242		46.8	0.071		138.0	0.196	
		0.325	±9/2		0.523	±13/2		0.269	±11/2
		19.231			17.256			18.771	
3	210.4	9.667		190.7	2.589		239.8	2.402	
		8.363	±11/2		4.706	±9/2		4.048	±13/2
		3.314			12.763			12.136	
4	248.3	0.905		248.9	8.268		292.1	2.068	
		2.960	±5/2		5.937	±7/2		5.756	±5/2
		10.123			2.488			9.485	
5	310.1	1.147		327.3	1.396		354.3	1.578	
		3.797	±3/2		3.360	±3/2		4.417	±3/2
		11.657			11.655			11.250	

6	384.0	1.055 1.607 15.143	$\pm 1/2$	425.5	0.779 1.261 14.958	$\pm 1/2$	418.5	0.811 1.336 15.654	$\pm 1/2$
7	438.0	0.194 0.330 18.875	$\pm 7/2$	525.4	0.183 0.258 18.470	$\pm 5/2$	510.3	0.181 0.322 18.756	$\pm 7/2$
8	640.8	0.018 0.023 19.791	$\pm 13/2$	753.8	0.015 0.022 19.779	$\pm 11/2$	664.5	0.029 0.055 19.699	$\pm 9/2$
KDs	3a_Dy5			3a_Dy6			3b_Dy1		
	E/cm^{-1}	g	m_J	E/cm^{-1}	g	m_J	E/cm^{-1}	g	m_J
1	0.0	0.000 0.001 19.675	$\pm 15/2$	0.0	0.002 0.003 19.656	$\pm 15/2$	0.0	0.038 0.087 19.636	
2	214.6	0.137 0.160 16.589	$\pm 13/2$	182.7	0.086 0.100 16.572	$\pm 13/2$	95.1	0.232 0.330 18.580	$\pm 13/2$
3	359.3	1.586 3.122 11.862	$\pm 11/2$	315.6	0.645 0.839 13.344	$\pm 11/2$	215.4	2.767 5.474 11.511	$\pm 9/2$
4	420.7	1.539 2.000 14.116	$\pm 3/2$	390.8	3.572 4.562 11.827	$\pm 7/2$	274.8	8.149 5.601 1.668	$\pm 5/2$
5	467.3	1.365 2.669 11.586	$\pm 9/2$	428.5	2.164 3.880 8.005	$\pm 3/2$	361.8	1.777 3.600 11.485	$\pm 3/2$
6	518.2	8.357 6.534 3.444	$\pm 7/2$	500.5	0.710 5.231 9.805	$\pm 5/2$	458.8	0.591 1.009 15.336	$\pm 1/2$
7	568.0	1.594 3.164 13.937	$\pm 5/2$	559.9	1.611 2.716 12.465	$\pm 9/2$	556.5	0.152 0.228 18.721	$\pm 7/2$
8	634.0	0.126 0.362 19.215	$\pm 1/2$	600.4	0.597 2.360 17.339	$\pm 1/2$	759.0	0.018 0.029 19.784	$\pm 11/2$
KDs	3b_Dy2			3b_Dy3			3b_Dy4		
	E/cm^{-1}	g	m_J	E/cm^{-1}	g	m_J	E/cm^{-1}	g	m_J
1	0.0	0.027 0.058 19.729	$\pm 15/2$	0.0	0.014 0.025 19.783	$\pm 15/2$	0.0	0.079 0.203 19.545	
2	110.3	0.265 0.394 18.686	$\pm 9/2$	138.9	0.368 0.557 18.728	$\pm 9/2$	67.5	0.190 0.380 18.914	$\pm 11/2$
3	217.1	9.305 8.271	$\pm 11/2$	234.0	3.603 6.694	$\pm 13/2$	187.1	3.197 5.673	$\pm 7/2$

		3.294			10.872			12.586	
4	264.4	0.712	$\pm 5/2$	289.4	1.119	$\pm 5/2$	237.4	1.817	$\pm 5/2$
		3.634			4.571			4.701	
		9.330			8.301			8.934	
5	338.0	1.687	$\pm 3/2$	362.8	1.730	$\pm 1/2$	313.4	0.700	$\pm 3/2$
		3.707			3.760			2.747	
		11.693			12.190			11.796	
6	422.0	0.637	$\pm 1/2$	443.2	0.540	$\pm 3/2$	397.4	0.796	$\pm 1/2$
		1.089			1.109			1.198	
		15.240			15.205			15.909	
7	501.5	0.164	$\pm 7/2$	553.3	0.171	$\pm 7/2$	478.2	0.184	$\pm 9/2$
		0.239			0.227			0.275	
		18.670			18.649			18.859	
8	715.8	0.015	$\pm 13/2$	716.9	0.026	$\pm 11/2$	643.6	0.032	$\pm 13/2$
		0.022			0.044			0.052	
		19.774			19.630			19.695	
KDs		3b_Dy5			3b_Dy6				
		E/cm^{-1}	g	m_J	E/cm^{-1}	g	m_J		
1	0.0	0.000		$\pm 15/2$	0.0	0.003			
		0.001				0.004			
		19.635				19.622			
2	192.7	0.189	$\pm 13/2$		173.9	0.084			
		0.205				0.101			
		16.361				16.569			
3	312.0	2.141	$\pm 11/2$		309.4	0.557			
		3.657				0.579			
		11.381				13.537			
4	370.5	1.482	$\pm 3/2$		407.8	2.945			
		2.908				4.655			
		11.573				8.998			
5	413.0	2.607	$\pm 9/2$		450.0	10.602			
		4.015				6.559			
		10.160				0.333			
6	472.3	3.534	$\pm 7/2$		510.6	1.263			
		4.192				4.942			
		6.740				9.627			
7	514.1	9.445	$\pm 5/2$		576.5	0.929			
		7.756				2.802			
		2.700				11.589			
8	570.5	0.296	$\pm 1/2$		616.0	0.682			
		0.994				2.886			
		18.634				16.286			

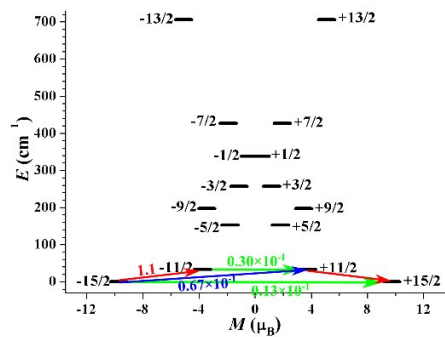
Table S15. Wave functions with definite projection of the total moment $|m_J\rangle$ for the lowest two KDs of individual Dy^{III} fragments for **1–3** using CASSCF/RASSI-SO with MOLCAS 8.4.

	E/cm^{-1}	wave functions
1_Dy1	0.0	94% $ \pm 15/2\rangle$
	54.5	10% $ \pm 9/2\rangle + 23\% \pm 7/2\rangle + 22\% \pm 5/2\rangle + 21\% \pm 3/2\rangle + 17\% \pm 1/2\rangle$
2_Dy1	0.0	94% $ \pm 15/2\rangle$
	48.3	13% $ \pm 9/2\rangle + 23\% \pm 7/2\rangle + 20\% \pm 5/2\rangle + 18\% \pm 3/2\rangle + 15\% \pm 1/2\rangle$
3a_Dy1	0.0	96% $ \pm 15/2\rangle$
	33.8	15% $ \pm 9/2\rangle + 18\% \pm 7/2\rangle + 20\% \pm 5/2\rangle + 18\% \pm 3/2\rangle + 15\% \pm 1/2\rangle$
3a_Dy2	0.0	99% $ \pm 15/2\rangle$
	110.0	15% $ \pm 9/2\rangle + 16\% \pm 7/2\rangle + 19\% \pm 5/2\rangle + 17\% \pm 3/2\rangle + 16\% \pm 1/2\rangle$
3a_Dy3	0.0	87% $ \pm 15/2\rangle$
	46.8	22% $ \pm 13/2\rangle + 10\% \pm 11/2\rangle + 17\% \pm 9/2\rangle + 14\% \pm 7/2\rangle + 13\% \pm 5/2\rangle + 10\% \pm 3/2\rangle$
3a_Dy4	0.0	99% $ \pm 15/2\rangle$
	138.0	17% $ \pm 13/2\rangle + 12\% \pm 11/2\rangle + 19\% \pm 9/2\rangle + 15\% \pm 7/2\rangle + 15\% \pm 5/2\rangle + 12\% \pm 3/2\rangle + 10\% \pm 1/2\rangle$
3a_Dy5	0.0	97% $ \pm 15/2\rangle$
	214.6	91% $ \pm 13/2\rangle$
3a_Dy6	0.0	96% $ \pm 15/2\rangle$
	182.7	90% $ \pm 13/2\rangle$
3b_Dy1	0.0	98% $ \pm 15/2\rangle$
	95.1	15% $ \pm 13/2\rangle + 11\% \pm 11/2\rangle + 17\% \pm 9/2\rangle + 15\% \pm 7/2\rangle + 15\% \pm 5/2\rangle + 13\% \pm 3/2\rangle + 12\% \pm 1/2\rangle$
3b_Dy2	0.0	98% $ \pm 15/2\rangle$
	110.3	12% $ \pm 13/2\rangle + 16\% \pm 9/2\rangle + 15\% \pm 7/2\rangle + 17\% \pm 5/2\rangle + 16\% \pm 3/2\rangle + 15\% \pm 1/2\rangle$
3b_Dy3	0.0	99% $ \pm 15/2\rangle$
	138.9	11% $ \pm 13/2\rangle + 14\% \pm 9/2\rangle + 14\% \pm 7/2\rangle + 17\% \pm 5/2\rangle + 18\% \pm 3/2\rangle + 18\% \pm 1/2\rangle$
3b_Dy4	0.0	97% $ \pm 15/2\rangle$
	67.5	15% $ \pm 9/2\rangle + 15\% \pm 7/2\rangle + 18\% \pm 5/2\rangle + 18\% \pm 3/2\rangle + 17\% \pm 1/2\rangle$
3b_Dy5	0.0	96% $ \pm 15/2\rangle$
	192.7	88% $ \pm 13/2\rangle + 10\% \pm 9/2\rangle$
3b_Dy6	0.0	96% $ \pm 15/2\rangle$
	173.9	90% $ \pm 13/2\rangle$

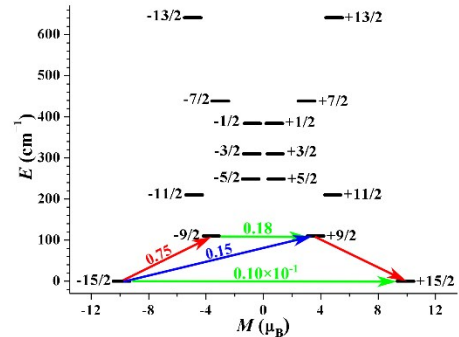


1_Dy1

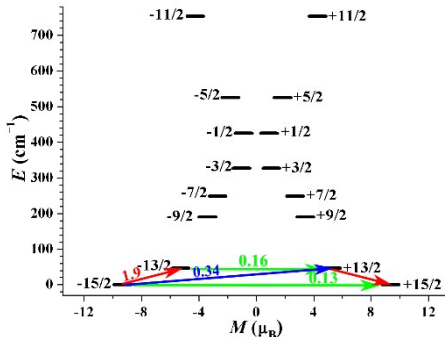
2_Dy1



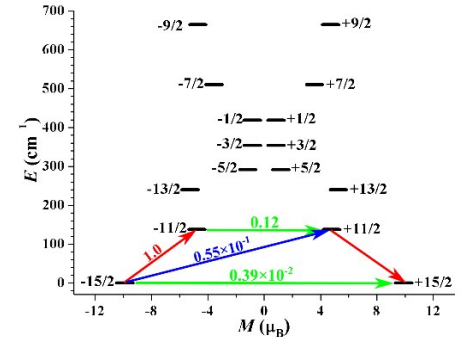
3a_Dy1



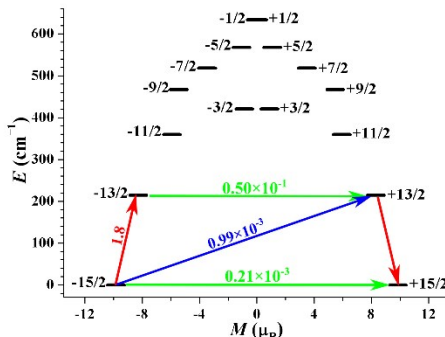
3a_Dy2



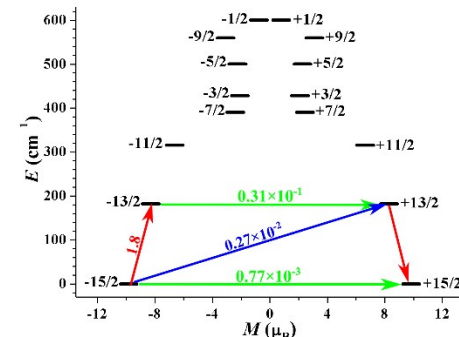
3a_Dy3



3a_Dy4



3a_Dy5



3a_Dy6

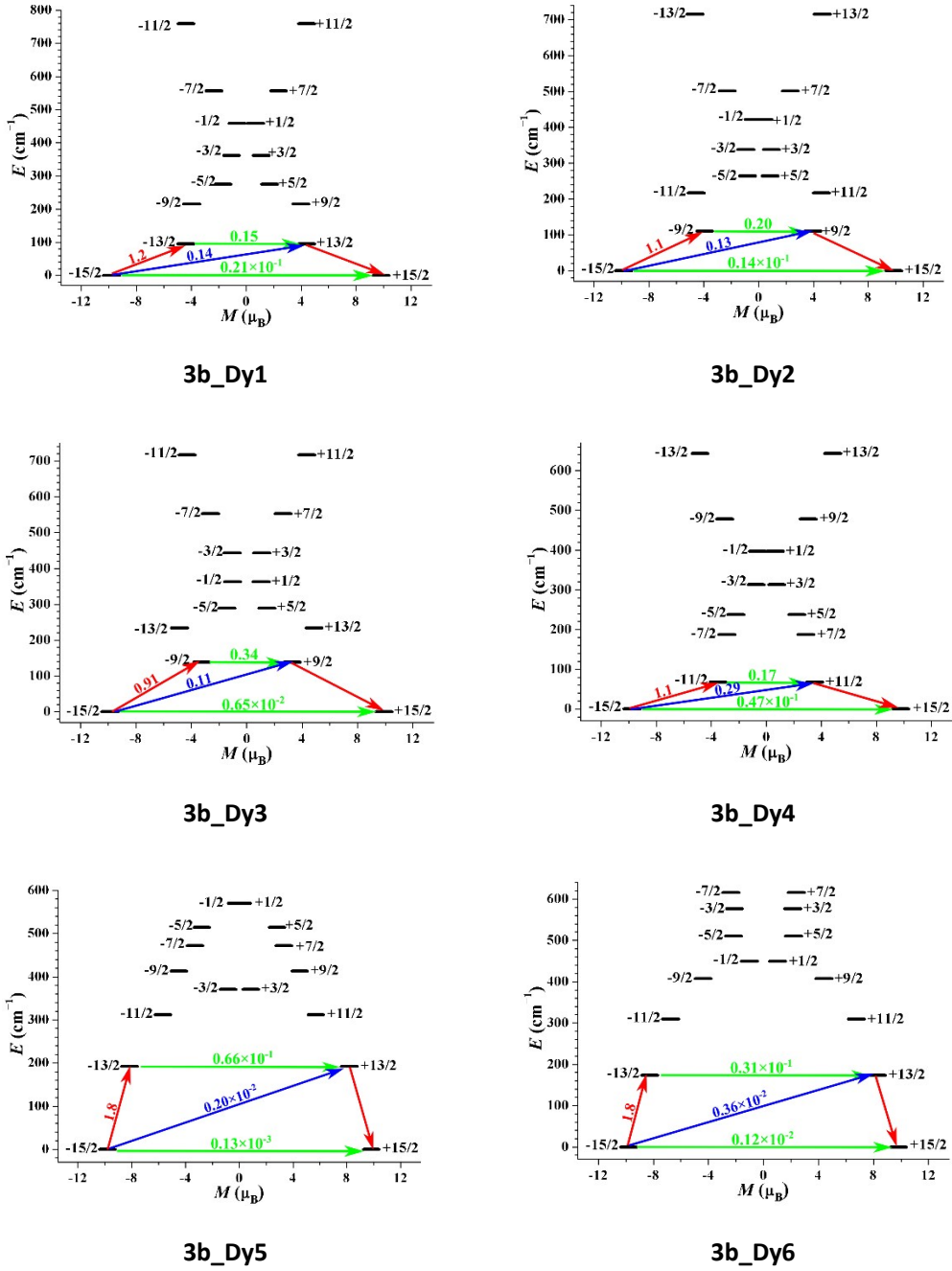


Figure S14. Magnetization blocking barriers for individual Dy^{III} fragments in **1–3**. The thick black lines represent the KDs of the individual Dy^{III} fragments as a function of their magnetic moment along the magnetic axis. The green lines correspond to diagonal matrix element of the transversal magnetic moment; the blue line represent Orbach relaxation processes. The path shown by the red arrows represents the most probable path for magnetic relaxation in the corresponding compounds. The numbers at each arrow stand for the mean absolute value of the corresponding matrix element of transition magnetic moment.

To fit the exchange interactions between Dy^{III} ions in **1** and **2**, we took two steps to obtain them. Firstly, we calculated individual Dy^{III} fragments using CASSCF/RASSI-SO to obtain the corresponding magnetic properties. Then, the exchange interactions between the magnetic centers are considered within the Lines model,^{S4} while the account of the dipole-dipole magnetic couplings are treated exactly. The Lines model is effective and has been successfully used widely in the research field of *d* and *f*-elements single-molecule magnets.^{S5} The Ising exchange Hamiltonians is:

$$\hat{H}_{exch} = -\tilde{J} \hat{\tilde{S}}_{Dy1} \hat{\tilde{S}}_{Dy2} \quad (1)$$

The $\tilde{J} = 25\cos\varphi J$, where φ is the angle between the anisotropy axes on sites Dy1 and Dy2, and J is the Lines exchange coupling parameter. The $\frac{g}{2} = 1/2$ is the ground pseudospin on the Dy^{III} site. The total \tilde{J}_{total} is the parameter of the total magnetic interaction ($\tilde{J}_{total} = \tilde{J}_{dipolar} + \tilde{J}_{exchange}$) between magnetic center ions. The dipolar magnetic couplings can be calculated exactly, while the Lines exchange coupling constants J were fitted through comparison of the computed and measured magnetic susceptibilities using the POLY_ANISO program.^{S3}

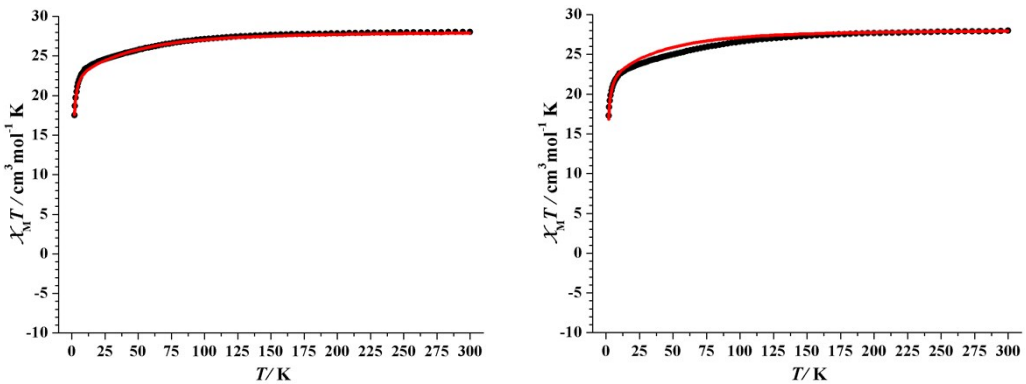


Figure S15. Calculated (red solid line) and experimental (black circle dot) data of magnetic susceptibilities of **1** (left) and **2** (right).

Table S16. Relevant parameters for the calculation of intermolecular magnetic interactions of **1** and **2**.

	g1z	g2z	r1	θ	ψ_1	ψ_2
$J_{1\text{dip}}$	19.318	19.318	7.788	0	54.396	54.396
$J_{2\text{dip}}$	19.255	19.255	7.832	0	57.676	57.676

Table S17. Exchange energies E (cm^{-1}), the energy difference between each exchange doublets Δ_t (cm^{-1}) and the main values of the g_z for the lowest two exchange doublets of **1–2**.

	1			2		
	E	Δ_t	g_z	E	Δ_t	g_z
1	0.0	5.57×10^{-4}	0.000	0.0	7.40×10^{-4}	0.000
2	0.8	6.06×10^{-4}	38.634	0.9	8.37×10^{-4}	38.493

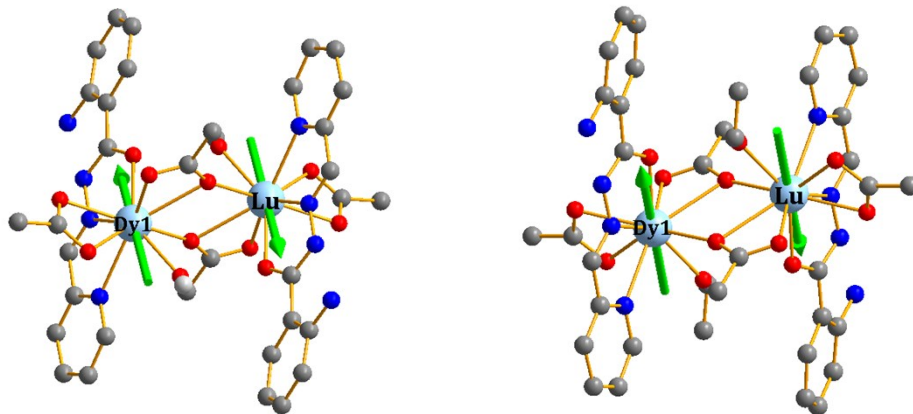
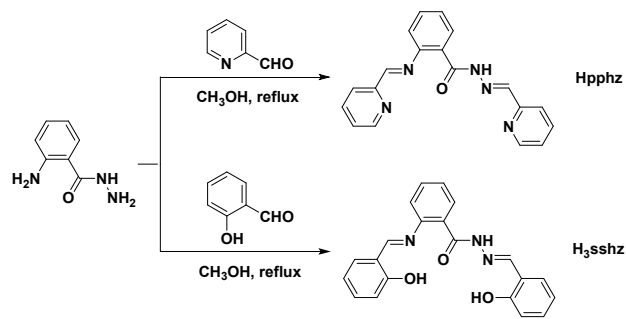


Figure S16. Calculated orientations of the local main magnetic axes on Dy^{III} ions of **1** (left) and **2** (right) in the ground KDs

References:

- S1 F. Aquilante, J. Autschbach, R. K. Carlson, L. F. Chibotaru, M. G. Delcey, L. De Vico, I. Fdez. Galván, N. Ferré, L. M. Frutos, L. Gagliardi, M. Garavelli, A. Giussani, C. E. Hoyer, G. Li Manni, H. Lischka, D. Ma, P. Å. Malmqvist, T. Müller, A. Nenov, M. Olivucci, T. B. Pedersen, D. Peng, F. Plasser, B. Pritchard, M. Reiher, I. Rivalta, I. Schapiro, J. Segarra-Martí, M. Stenrup, D. G. Truhlar, L. Ungur, A. Valentini, S. Vancoillie, V. Veryazov, V. P. Vysotskiy, O. Weingart, F. Zapata and R. Lindh, *J. Comput. Chem.*, 2016, **37**, 506.
- S2 L. Seijo and Z. Barandiarán, *Computational Chemistry: Reviews of Current Trends*; World Scientific, Inc.:

- Singapore, 1999; pp 455–152.
- S3 (a) L. F. Chibotaru, L. Ungur, A. Soncini, *Angew. Chem. Int. Ed.*, 2008, **47**, 4126. (b) L. Ungur, W. Van den Heuvel, L. F. Chibotaru, *New J. Chem.*, 2009, **33**, 1224. (c) L. F. Chibotaru, L. Ungur, C. Aronica, H. Elmoll, G. Pilet and D. Luneau, *J. Am. Chem. Soc.*, 2008, **130**, 12445.
- S4 M. E. Lines, *J. Chem. Phys.*, 1971, **55**, 2977.
- S5 (a) K. C. Mondal, A. Sundt, Y. H. Lan, G. E. Kostakis, O. Waldmann, L. Ungur, L. F. Chibotaru, C. E. Anson, A. K. Powell, *Angew. Chem. Int. Ed.*, 2012, **51**, 7550. (b) S. K. Langley, D. P. Wielechowski, V. Vieru, N. F. Chilton, B. Moubaraki, B. F. Abrahams, L. F. Chibotaru and K. S. Murray, *Angew. Chem. Int. Ed.*, 2013, **52**, 12014.



Scheme S1. Synthetic route of the Hpphz and H₃sshz ligands.

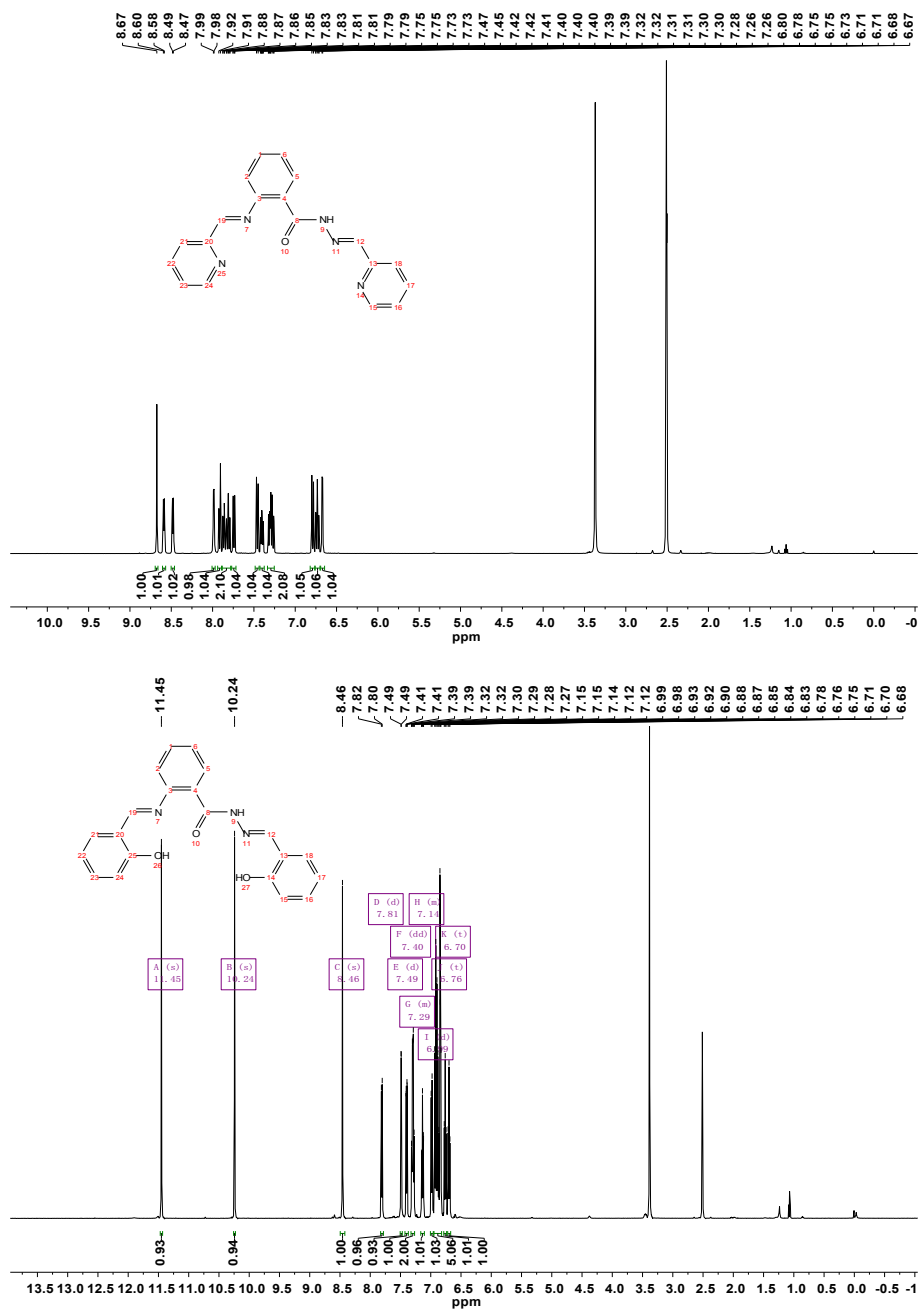


Figure S17. ¹H NMR of the Hpphz (top) and H₃sshz (down) ligands.

Table S18. Dy^{III} and Y^{III} ion contents of **1@Y** and **2@Y** determined by energy dispersive spectroscope (EDS) of field-emission scanning electron microscope.

Sample	element	first time/%	second time/%	third time/%	mean value/%
1@Y	Dy	11.38	10.15	11.07	10.83
	Y	88.62	89.85	88.93	89.07
2@Y	Dy	7.93	7.55	9.66	8.38
	Y	92.07	92.45	90.34	91.62

Table S19. Crystal data and structure refinement parameters for **1-3**.

Identification	1	2	3
Formula	C ₃₆ H ₄₂ Dy ₂ N ₈ O ₁₂	C ₃₈ H ₄₆ Dy ₂ N ₈ O ₁₂	C _{193.5} H ₂₂₆ Dy ₁₂ N ₂₄ O _{61.5}
Fw	1103.77	1131.83	5826.97
Temp./K	298.15	302.13	150.0
Crystal system	triclinic	triclinic	monoclinic
Space group	<i>P</i> 1	<i>P</i> 1	<i>P</i> 2 ₁ /n
<i>a</i> /Å	9.4383(5)	9.4259(4)	24.8663(1)
<i>b</i> /Å	10.7965(6)	10.7569(3)	25.6934(1)
<i>c</i> /Å	11.0469(4)	11.1938(3)	33.2952(2)
<i>α</i> /°	109.736(4)	109.174(3)	90
<i>β</i> /°	100.143(4)	100.065(3)	94.804(2)
<i>γ</i> /°	90.382(5)	90.1607(3)	90
V/Å ³	1040.34(9)	1053.30(6)	21197.6(2)
Z	1	1	4
<i>D</i> _v /g cm ⁻³	1.762	1.784	1.824
<i>m</i> μ/mm ⁻¹	3.632	3.590	4.258
<i>F</i> (000)	542	558	11354
Reflns collected	6680	14369	232949
<i>R</i> _{int}	0.0257	0.0540	0.0956
GOF	1.050	1.044	1.090
<i>R</i> ₁ , <i>wR</i> ₂ (<i>I</i> > 2σ(<i>I</i>)) ^a	0.027, 0.052	0.034, 0.085	0.054, 0.120
<i>R</i> ₁ , <i>wR</i> ₂ (all data) ^b	0.032, 0.055	0.039, 0.087	0.098, 0.148

$${}^a R_1 = \sum \frac{\|F_o\| - |F_c\|}{\sum |F_o|}, {}^b wR_2 = [\sum w(|F_o^2| - |F_c^2|)^2 / \sum w(|F_o^2|)^2]^{1/2}$$

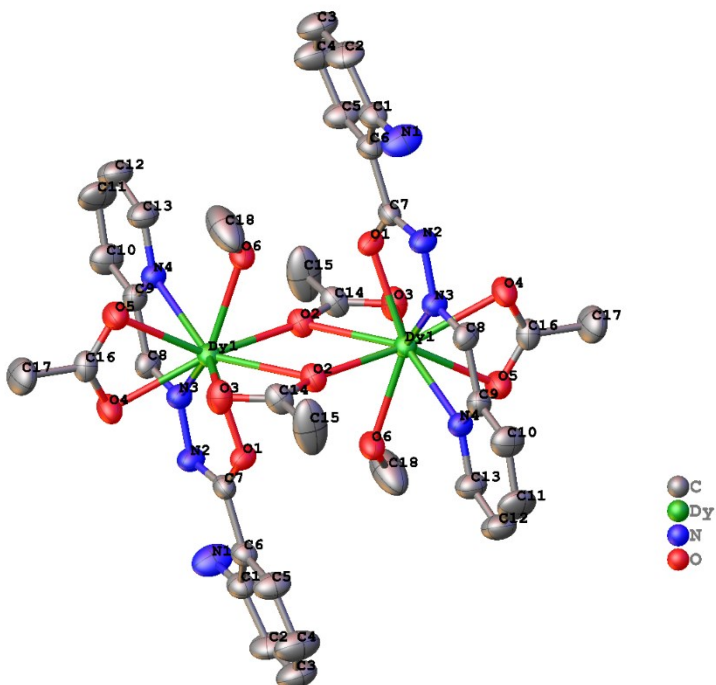


Figure S18. Perspective ORTEP drawing of **1** (the hydrogen atoms were omitted for clarity).

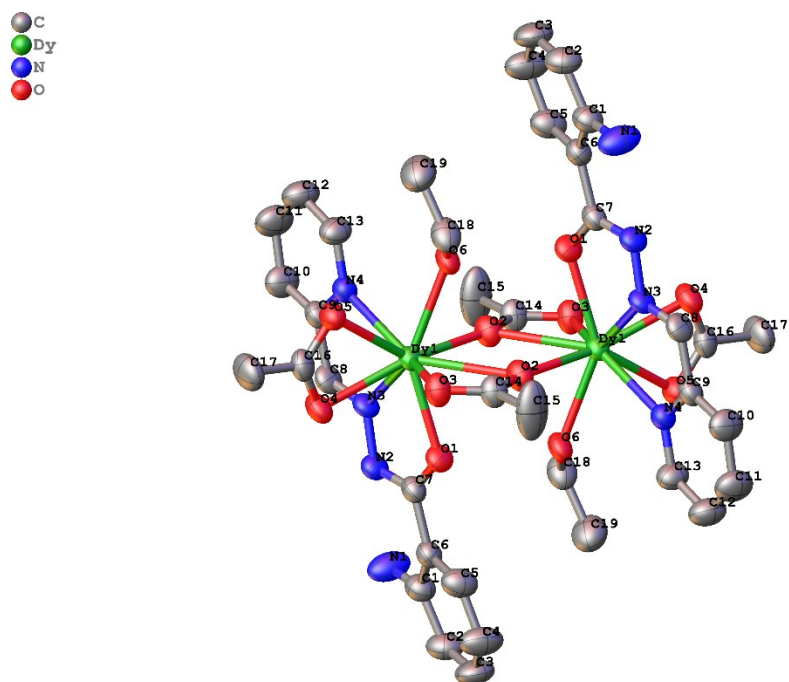


Figure S19. Perspective ORTEP drawing of **2** (the hydrogen atoms were omitted for clarity).

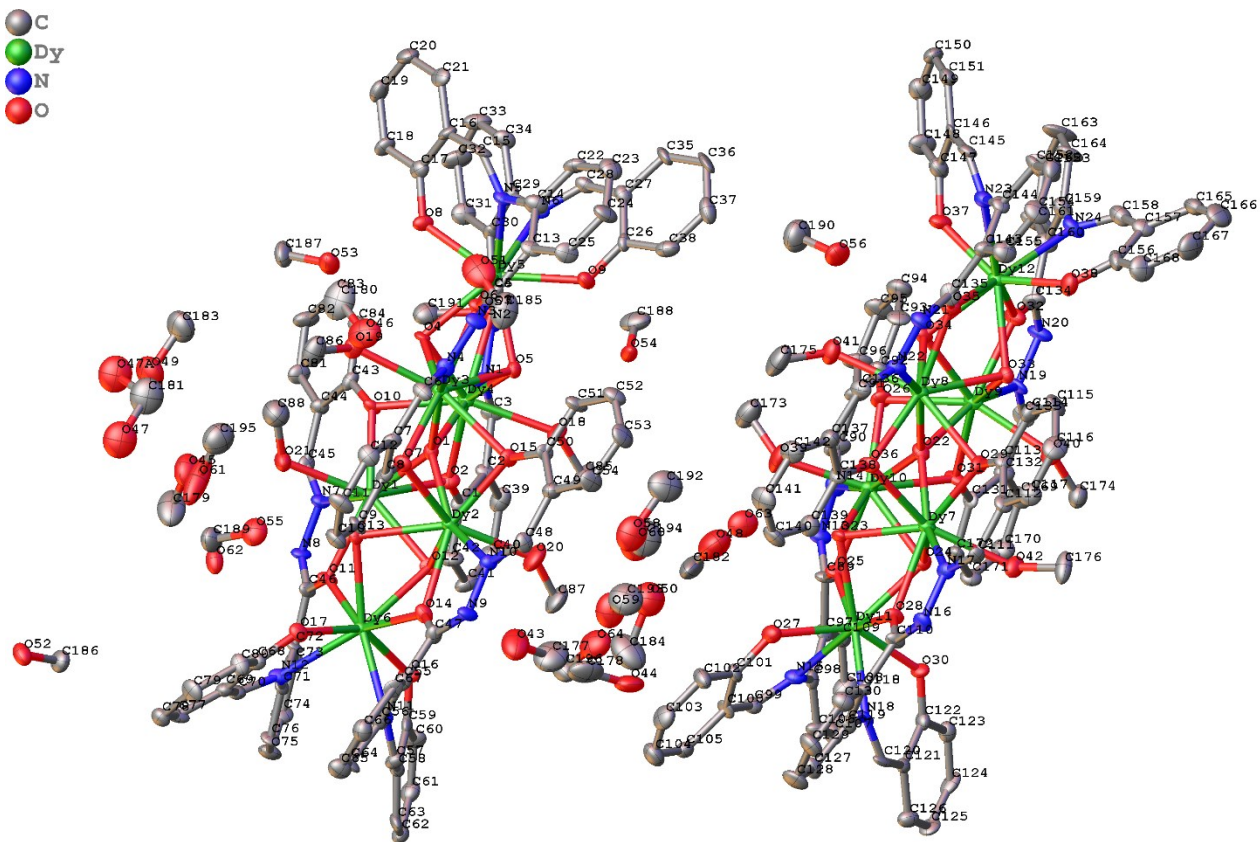


Figure S20. Perspective ORTEP drawing of **3** (the hydrogen atoms were omitted for clarity).

Table S20. Selected bond lengths (Å) and angles (°) for **1**.

Bond	Length (Å)	Bond	Length (Å)	Bond	Length (Å)
Dy1—O1	2.337(3)	Dy1—O5	2.462(3)	Dy1—O3	2.418(3)
Dy1—O2	2.346(3)	Dy1—O6	2.416(3)	Dy1—O4	2.388(3)
Dy1—O2a	2.639(2)	Dy1—N3	2.483(3)	Dy1—N4	2.590(3)
Bond Angle	Angle (°)	Bond Angle	Angle (°)	Bond Angle	Angle (°)
O1—Dy1—O2	84.27(9)	O3—Dy1—O5	74.55(1)	O2—Dy1—N3	82.49(1)
O1—Dy1—O2a	71.71(8)	O3—Dy1—N3	137.04(1)	O2—Dy1—N4	83.23(1)
O1—Dy1—O3	80.64(9)	O3—Dy1—N4	148.89(1)	O4—Dy1—O2a	125.81(9)
O1—Dy1—O4	81.95(9)	N3—Dy1—O2a	127.63(1)	O4—Dy1—O3	78.89(1)
O1—Dy1—O5	132.13(1)	N3—Dy1—N4	63.33(1)	O4—Dy1—O5	53.68(9)
O1—Dy1—O6	143.29(9)	N4—Dy1—O2a	144.33(9)	O4—Dy1—O6	128.45(1)
O1—Dy1—N3	63.40(1)	O5—Dy1—O2a	117.68(9)	O4—Dy1—N3	73.74(1)
O1—Dy1—N4	126.37(9)	O5—Dy1—N3	112.15(9)	O4—Dy1—N4	89.19(1)
O2—Dy1—O2a	67.11(1)	O5—Dy1—N4	75.24(9)	O6—Dy1—N3	137.35(1)
O2—Dy1—O3	118.12(9)	O6—Dy1—O2a	73.15(9)	O6—Dy1—N4	79.52(1)
O2—Dy1—O4	155.96(1)	O6—Dy1—O3	85.60(9)	O3—Dy1—O2a	51.13(8)
O2—Dy1—O5	143.59(1)	O6—Dy1—O5	74.85(9)	O2—Dy1—O6	72.56(9)

a: $-x+1, -y+1, -z+1$.**Table S21.** Selected bond lengths (Å) and angles (°) for **2**.

Bond	Length (Å)	Bond	Length (Å)	Bond	Length (Å)
Dy1—O1	2.339(4)	Dy1—O3a	2.409(4)	Dy1—O6	2.422(3)
Dy1—O2a	2.667(4)	Dy1—O4	2.396(3)	Dy1—N3	2.477(4)
Dy1—O2	2.345(3)	Dy1—O5	2.445(3)	Dy1—N4	2.583(4)
Bond Angle	Angle (°)	Bond Angle	Angle (°)	Bond Angle	Angle (°)
O1—Dy1—O2	85.34(1)	O2—Dy1—N3	83.01(1)	O4—Dy1—N4	88.38(1)
O1—Dy1—O2a	71.93(1)	O2—Dy1—N4	83.58(1)	O5—Dy1—O2a	116.66(1)
O1—Dy1—O3a	80.46(1)	O3a—Dy1—O2a	50.46(1)	O5—Dy1—N3	112.42(1)
O1—Dy1—O4	81.73(1)	O3a—Dy1—O5	74.15(1)	O5—Dy1—N4	75.20(1)
O1—Dy1—O5	131.75(1)	O3a—Dy1—O6	85.06(1)	O6—Dy1—O2a	72.97(1)
O1—Dy1—O6	143.46(1)	O3a—Dy1—N3	137.37(1)	O6—Dy1—O5	74.36(1)
O1—Dy1—N3	63.80(1)	O3a—Dy1—N4	148.57(1)	O6—Dy1—N3	137.55(1)
O1—Dy1—N4	126.45(1)	O4—Dy1—O2a	125.52(1)	O6—Dy1—N4	80.17(1)
O2—Dy1—O3a	117.99(1)	O4—Dy1—O3a	79.16(1)	N3—Dy1—O2 ^a	128.31(1)
O2—Dy1—O4	156.46(1)	O4—Dy1—O5	53.83(1)	N3—Dy1—N4	62.91(1)
O2—Dy1—O5	142.87(1)	O4—Dy1—O6	128.12(1)	N4—Dy1—O2a	145.30(1)
O2—Dy1—O6	72.21(1)	O4—Dy1—N3	73.64(1)	Dy1—O2—Dy1a	112.30(1)

a: $-x+1, -y+1, -z+1$.

Table S22. Selected bond lengths (\AA) and angles ($^\circ$) for **3**.

Bond	Length (\AA)	Bond	Length (\AA)	Bond	Length (\AA)
Dy1—O1	2.296(6)	Dy5—O3	2.365(6)	Dy9—O22	2.257(7)
Dy1—O2	2.421(7)	Dy5—O4	2.380(6)	Dy9—O26	2.466(7)
Dy1—O10	2.351(6)	Dy5—O5	2.369(7)	Dy9—O31	2.357(6)
Dy1—O11	2.356(6)	Dy5—O6	2.366(6)	Dy9—O32	2.357(7)
Dy1—O12	2.378(7)	Dy5—O8	2.254(7)	Dy9—O33	2.341(6)
Dy1—O13	2.319(6)	Dy5—O9	2.253(7)	Dy9—O34	2.379(7)
Dy1—O21	2.393(7)	Dy5—N5	2.516(8)	Dy9—O40	2.361(8)
Dy1—N7	2.485(8)	Dy5—N6	2.510(8)	Dy9—N19	2.499(8)
Dy2—O1	2.284(6)	Dy6—O11	2.384(6)	Dy10—O22	2.271(6)
Dy2—O7	2.440(6)	Dy6—O12	2.395(7)	Dy10—O23	2.328(6)
Dy2—O12	2.333(6)	Dy6—O13	2.376(6)	Dy10—O24	2.410(6)
Dy2—O13	2.431(6)	Dy6—O14	2.368(7)	Dy10—O25	2.367(6)
Dy2—O14	2.352(7)	Dy6—O16	2.234(7)	Dy10—O26	2.326(7)
Dy2—O15	2.335(7)	Dy6—O17	2.252(7)	Dy10—O31	2.406(7)
Dy2—O20	2.365(8)	Dy6—N11	2.499(8)	Dy10—O39	2.385(8)
Dy2—N10	2.482(8)	Dy6—N12	2.556(8)	Dy10—N14	2.490(8)
Dy3—O1	2.295(6)	Dy7—O22	2.263(7)	Dy11—O23	2.418(6)
Dy3—O4	2.329(6)	Dy7—O23	2.434(7)	Dy11—O24	2.346(7)
Dy3—O5	2.422(7)	Dy7—O24	2.314(6)	Dy11—O25	2.359(7)
Dy3—O6	2.349(6)	Dy7—O28	2.366(6)	Dy11—O27	2.260(7)
Dy3—O7	2.319(6)	Dy7—O29	2.316(7)	Dy11—O28	2.349(6)
Dy3—O15	2.409(7)	Dy7—O36	2.448(7)	Dy11—O30	2.267(7)
Dy3—O19	2.414(7)	Dy7—O42	2.406(7)	Dy11—N15	2.534(8)
Dy3—N4	2.494(8)	Dy7—N17	2.462(8)	Dy11—N18	2.493(8)
Dy4—O1	2.259(6)	Dy8—O22	2.275(6)	Dy12—O32	2.397(7)
Dy4—O2	2.336(7)	Dy8—O29	2.433(7)	Dy12—O33	2.376(6)
Dy4—O3	2.355(6)	Dy8—O33	2.405(6)	Dy12—O34	2.377(7)
Dy4—O4	2.413(6)	Dy8—O34	2.332(6)	Dy12—O35	2.371(7)
Dy4—O5	2.313(6)	Dy8—O35	2.348(7)	Dy12—O37	2.256(7)
Dy4—O10	2.406(7)	Dy8—O36	2.342(6)	Dy12—O38	2.210(8)
Dy4—O18	2.390(7)	Dy8—O41	2.421(8)	Dy12—N23	2.535(8)
Dy4—N1	2.494(8)	Dy8—N22	2.494(8)	Dy12—N24	2.554(9)
Bond Angle	Angle ($^\circ$)	Bond Angle	Angle ($^\circ$)	Bond Angle	Angle ($^\circ$)
O1—Dy1—O2	75.7(2)	O8—Dy5—N5	74.1(3)	O31—Dy9—O40	78.6(3)
O1—Dy1—O10	76.6(2)	O8—Dy5—N6	82.9(3)	O31—Dy9—N19	72.7(2)
O1—Dy1—O11	144.7(2)	O9—Dy5—O3	99.9(2)	O32—Dy9—O26	109.5(2)
O1—Dy1—O12	77.3(2)	O9—Dy5—O4	137.2(2)	O32—Dy9—O34	71.1(2)
O1—Dy1—O13	77.1(2)	O9—Dy5—O5	75.6(2)	O32—Dy9—O40	98.3(3)
O1—Dy1—O21	106.1(2)	O9—Dy5—O6	90.9(2)	O32—Dy9—N19	64.1(2)
O1—Dy1—N7	150.0(2)	O9—Dy5—O8	148.2(2)	O33—Dy9—O26	131.6(2)
O2—Dy1—N7	84.3(3)	O9—Dy5—N5	82.8(3)	O33—Dy9—O31	143.3(2)

O10—Dy1—O2	68.6(2)	O9—Dy5—N6	73.4(3)	O33—Dy9—O32	72.4(2)
O10—Dy1—O11	138.8(2)	N6—Dy5—N5	84.7(3)	O33—Dy9—O34	61.3(2)
O10—Dy1—O12	140.7(2)	O11—Dy6—O12	70.9(2)	O33—Dy9—O40	74.5(2)
O10—Dy1—O21	77.2(2)	O11—Dy6—N11	150.1(2)	O33—Dy9—N19	126.3(3)
O10—Dy1—N7	75.4(2)	O11—Dy6—N12	68.6(2)	O34—Dy9—O26	73.5(2)
O11—Dy1—O2	112.3(2)	O12—Dy6—N11	122.2(2)	O34—Dy9—N19	125.1(2)
O11—Dy1—O12	71.7(2)	O12—Dy6—N12	135.7(2)	O40—Dy9—O26	146.1(2)
O11—Dy1—O21	87.0(2)	O13—Dy6—O11	72.3(2)	O40—Dy9—O34	135.8(2)
O11—Dy1—N7	64.0(2)	O13—Dy6—O12	61.3(2)	O40—Dy9—N19	82.0(3)
O12—Dy1—O2	76.8(2)	O13—Dy6—N11	137.3(2)	O22—Dy10—O23	78.4(2)
O12—Dy1—O21	138.7(2)	O13—Dy6—N12	119.7(2)	O22—Dy10—O24	75.0(2)
O12—Dy1—N7	119.8(2)	O14—Dy6—O11	137.6(2)	O22—Dy10—O25	142.7(2)
O13—Dy1—O2	134.8(2)	O14—Dy6—O12	72.2(2)	O22—Dy10—O26	76.8(2)
O13—Dy1—O10	136.8(2)	O14—Dy6—O13	72.1(2)	O22—Dy10—O31	77.4(2)
O13—Dy1—O11	73.8(2)	O14—Dy6—N11	70.1(2)	O22—Dy10—O39	106.7(3)
O13—Dy1—O12	62.4(2)	O14—Dy6—N12	151.9(2)	O22—Dy10—N14	149.5(3)
O13—Dy1—O21	78.0(2)	O16—Dy6—O11	85.4(2)	O23—Dy10—O24	61.7(2)
O13—Dy1—N7	131.9(2)	O16—Dy6—O12	75.2(2)	O23—Dy10—O25	74.5(2)
O21—Dy1—O2	144.5(2)	O16—Dy6—O13	135.5(2)	O23—Dy10—O31	133.7(2)
O21—Dy1—N7	77.8(3)	O16—Dy6—O14	104.7(3)	O23—Dy10—O39	74.3(3)
O1—Dy2—O7	76.4(2)	O16—Dy6—O17	145.8(2)	O23—Dy10—N14	131.5(3)
O1—Dy2—O12	78.5(2)	O16—Dy6—N11	74.0(3)	O24—Dy10—N14	121.1(3)
O1—Dy2—O13	75.1(2)	O16—Dy6—N12	84.4(3)	O25—Dy10—O24	69.8(2)
O1—Dy2—O14	143.8(2)	O17—Dy6—O11	109.2(2)	O25—Dy10—O31	103.8(2)
O1—Dy2—O15	76.9(2)	O17—Dy6—O12	138.3(2)	O25—Dy10—O39	90.1(3)
O1—Dy2—O20	105.6(3)	O17—Dy6—O13	78.6(2)	O25—Dy10—N14	64.5(3)
O1—Dy2—N10	149.7(2)	O17—Dy6—O14	85.4(2)	O26—Dy10—O23	139.8(2)
O7—Dy2—N10	83.9(2)	O17—Dy6—N11	79.3(3)	O26—Dy10—O24	137.9(2)
O12—Dy2—O7	134.9(2)	O17—Dy6—N12	73.4(2)	O26—Dy10—O25	139.3(2)
O12—Dy2—O13	61.4(2)	N11—Dy6—N12	87.7(3)	O26—Dy10—O31	69.5(2)
O12—Dy2—O14	73.7(2)	Dy1—O1—Dy3	144.8(3)	O26—Dy10—O39	83.2(3)
O12—Dy2—O15	138.6(2)	Dy2—O1—Dy1	96.1(2)	O26—Dy10—N14	74.8(3)
O12—Dy2—O20	75.8(3)	Dy2—O1—Dy3	94.1(2)	O31—Dy10—O24	74.2(2)
O12—Dy2—N10	130.8(2)	Dy4—O1—Dy1	95.0(2)	O31—Dy10—N14	82.5(3)
O13—Dy2—O7	76.2(2)	Dy4—O1—Dy2	141.9(3)	O39—Dy10—O24	134.9(3)
O13—Dy2—N10	122.4(2)	Dy4—O1—Dy3	97.5(2)	O39—Dy10—O31	150.9(3)
O14—Dy2—Dy1	102.08(16)	Dy4—O2—Dy1	89.7(2)	O39—Dy10—N14	80.7(3)
O14—Dy2—O7	108.0(2)	Dy4—O3—Dy5	98.6(2)	O23—Dy11—N15	125.9(2)
O14—Dy2—O13	71.4(2)	Dy3—O4—Dy4	92.4(2)	O23—Dy11—N18	134.0(2)
O14—Dy2—O20	89.7(3)	Dy3—O4—Dy5	98.6(2)	O24—Dy11—O23	61.3(2)
O14—Dy2—N10	64.4(2)	Dy5—O4—Dy4	96.6(2)	O24—Dy11—O25	71.0(2)
O15—Dy2—O7	69.1(2)	Dy4—O5—Dy3	92.6(2)	O24—Dy11—O28	73.3(2)
O15—Dy2—O13	139.5(2)	Dy4—O5—Dy5	99.7(2)	O24—Dy11—N15	133.6(2)

O15—Dy2—O14	139.0(2)	Dy5—O5—Dy3	96.3(2)	O24—Dy11—N18	124.8(2)
O15—Dy2—O20	79.4(3)	Dy3—O6—Dy5	98.4(2)	O25—Dy11—O23	73.0(2)
O15—Dy2—N10	74.6(2)	Dy3—O7—Dy2	89.5(2)	O25—Dy11—N15	69.6(2)
O20—Dy2—O7	147.3(3)	Dy1—O10—Dy4	89.7(2)	O25—Dy11—N18	151.9(2)
O20—Dy2—O13	136.4(3)	Dy1—O11—Dy6	98.1(2)	O27—Dy11—O23	77.9(2)
O20—Dy2—N10	79.2(3)	Dy1—O12—Dy6	97.2(3)	O27—Dy11—O24	139.1(2)
O1—Dy3—O4	76.0(2)	Dy2—O12—Dy1	92.6(2)	O27—Dy11—O25	101.2(3)
O1—Dy3—O5	75.5(2)	Dy2—O12—Dy6	98.8(2)	O27—Dy11—O28	90.6(3)
O1—Dy3—O6	142.5(2)	Dy1—O13—Dy2	91.6(2)	O27—Dy11—O30	145.2(2)
O1—Dy3—O7	78.6(2)	Dy1—O13—Dy6	99.3(2)	O27—Dy11—N15	72.8(3)
O1—Dy3—O15	75.2(2)	Dy6—O13—Dy2	96.6(2)	O27—Dy11—N18	81.2(3)
O1—Dy3—O19	108.6(2)	Dy2—O14—Dy6	99.0(2)	O28—Dy11—O23	69.5(2)
O1—Dy3—N4	151.4(2)	Dy2—O15—Dy3	89.9(2)	O28—Dy11—O25	137.2(2)
O4—Dy3—O5	61.6(2)	O22—Dy7—O23	76.4(2)	O28—Dy11—N15	152.0(2)
O4—Dy3—O6	75.6(2)	O22—Dy7—O24	77.1(2)	O28—Dy11—N18	70.2(2)
O4—Dy3—O15	132.0(2)	O22—Dy7—O28	142.2(2)	O30—Dy11—O23	136.9(2)
O4—Dy3—O19	73.1(2)	O22—Dy7—O29	77.6(2)	O30—Dy11—O24	75.7(2)
O4—Dy3—N4	131.5(2)	O22—Dy7—O36	75.1(2)	O30—Dy11—O25	90.7(2)
O5—Dy3—N4	121.3(2)	O22—Dy7—O42	107.2(3)	O30—Dy11—O28	102.7(2)
O6—Dy3—O5	69.7(2)	O22—Dy7—N17	151.1(3)	O30—Dy11—N15	81.2(3)
O6—Dy3—O15	107.4(2)	O23—Dy7—O36	76.3(2)	O30—Dy11—N18	73.6(3)
O6—Dy3—O19	85.7(2)	O23—Dy7—N17	120.9(2)	N18—Dy11—N15	84.7(3)
O6—Dy3—N4	63.9(2)	O24—Dy7—O23	61.5(2)	O32—Dy12—N23	151.4(3)
O7—Dy3—O4	138.6(2)	O24—Dy7—O28	73.5(2)	O32—Dy12—N24	69.2(3)
O7—Dy3—O5	140.1(2)	O24—Dy7—O29	137.7(2)	O33—Dy12—O32	71.1(2)
O7—Dy3—O6	138.3(2)	O24—Dy7—O36	133.7(2)	O33—Dy12—O34	60.9(2)
O7—Dy3—O15	69.9(2)	O24—Dy7—O42	73.5(2)	O33—Dy12—N23	137.3(2)
O7—Dy3—O19	84.8(2)	O24—Dy7—N17	130.8(2)	O33—Dy12—N24	117.5(3)
O7—Dy3—N4	74.3(2)	O28—Dy7—O23	69.0(2)	O34—Dy12—O32	70.4(2)
O15—Dy3—O5	74.4(2)	O28—Dy7—O36	109.6(2)	O34—Dy12—N23	121.7(3)
O15—Dy3—O19	153.4(2)	O28—Dy7—O42	86.7(3)	O34—Dy12—N24	136.8(2)
O15—Dy3—N4	86.9(2)	O28—Dy7—N17	64.9(2)	O35—Dy12—O32	136.4(2)
O19—Dy3—O5	132.2(2)	O29—Dy7—O23	141.1(2)	O35—Dy12—O33	71.8(2)
O19—Dy3—N4	78.1(3)	O29—Dy7—O28	139.9(2)	O35—Dy12—O34	72.0(2)
O1—Dy4—O2	78.1(2)	O29—Dy7—O36	69.4(2)	O35—Dy12—N23	70.0(3)
O1—Dy4—O3	142.8(2)	O29—Dy7—O42	82.4(2)	O35—Dy12—N24	151.2(3)
O1—Dy4—O4	75.1(2)	O29—Dy7—N17	75.1(3)	O37—Dy12—Dy8	108.38(19)
O1—Dy4—O5	78.4(2)	O36—Dy7—N17	86.2(2)	O37—Dy12—Dy9	100.26(17)
O1—Dy4—O10	76.2(2)	O42—Dy7—O23	133.0(2)	O37—Dy12—O32	86.1(3)
O1—Dy4—O18	103.2(3)	O42—Dy7—O36	150.6(2)	O37—Dy12—O33	136.1(2)
O1—Dy4—N1	151.8(2)	O42—Dy7—N17	78.7(3)	O37—Dy12—O34	76.5(2)
O2—Dy4—O3	138.3(2)	O22—Dy8—O29	75.0(2)	O37—Dy12—O35	105.9(3)
O2—Dy4—O4	140.1(2)	O22—Dy8—O33	77.4(2)	O37—Dy12—N23	73.4(3)

O2—Dy4—O10	69.1(2)	O22—Dy8—O34	77.1(2)	O37—Dy12—N24	86.1(3)
O2—Dy4—O18	81.3(2)	O22—Dy8—O35	144.6(2)	O38—Dy12—Dy8	100.8(2)
O2—Dy4—N1	74.7(2)	O22—Dy8—O36	77.0(2)	O38—Dy12—Dy9	113.2(2)
O3—Dy4—O4	69.8(2)	O22—Dy8—O41	100.7(3)	O38—Dy12—O32	111.3(3)
O3—Dy4—O10	106.3(2)	O22—Dy8—N22	151.3(2)	O38—Dy12—O33	79.6(3)
O3—Dy4—O18	92.3(3)	O29—Dy8—N22	92.0(2)	O38—Dy12—O34	138.1(2)
O3—Dy4—N1	63.7(2)	O33—Dy8—O29	74.0(2)	O38—Dy12—O35	83.4(3)
O4—Dy4—N1	123.3(2)	O33—Dy8—O41	132.8(2)	O38—Dy12—O37	144.2(3)
O5—Dy4—O2	139.1(2)	O33—Dy8—N22	124.2(2)	O38—Dy12—N23	77.9(3)
O5—Dy4—O3	74.5(2)	O34—Dy8—O29	131.1(2)	O38—Dy12—N24	72.5(3)
O5—Dy4—O4	61.9(2)	O34—Dy8—O33	61.1(2)	N23—Dy12—N24	89.3(3)
O5—Dy4—O10	135.1(2)	O34—Dy8—O35	73.2(2)	Dy7—O22—Dy8	95.7(2)
O5—Dy4—O18	72.1(2)	O34—Dy8—O36	139.8(2)	Dy7—O22—Dy10	97.5(2)
O5—Dy4—N1	128.0(3)	O34—Dy8—O41	72.4(3)	Dy9—O22—Dy7	139.4(3)
O10—Dy4—O4	76.0(2)	O34—Dy8—N22	128.3(2)	Dy9—O22—Dy8	96.5(2)
O10—Dy4—N1	87.3(2)	O35—Dy8—O29	111.3(2)	Dy9—O22—Dy10	95.6(2)
O18—Dy4—O4	133.5(2)	O35—Dy8—O33	71.6(2)	Dy10—O22—Dy8	142.9(3)
O18—Dy4—O10	149.9(2)	O35—Dy8—O41	88.4(3)	Dy10—O23—Dy7	91.4(2)
O18—Dy4—N1	79.9(3)	O35—Dy8—N22	63.9(2)	Dy10—O23—Dy11	98.2(2)
O3—Dy5—O4	70.2(2)	O36—Dy8—O29	69.3(2)	Dy11—O23—Dy7	95.8(2)
O3—Dy5—O5	73.3(2)	O36—Dy8—O33	139.4(2)	Dy7—O24—Dy10	92.3(2)
O3—Dy5—O6	137.9(2)	O36—Dy8—O35	138.3(2)	Dy7—O24—Dy11	101.1(3)
O3—Dy5—N5	152.1(2)	O36—Dy8—O41	82.8(3)	Dy11—O24—Dy10	98.0(3)
O3—Dy5—N6	69.8(2)	O36—Dy8—N22	74.4(2)	Dy11—O25—Dy10	98.8(2)
O4—Dy5—N5	125.5(2)	O41—Dy8—O29	152.1(3)	Dy10—O26—Dy9	88.8(2)
O4—Dy5—N6	133.1(2)	O41—Dy8—N22	78.7(3)	Dy11—O28—Dy7	99.5(2)
O5—Dy5—O4	61.6(2)	O22—Dy9—O26	74.3(2)	Dy7—O29—Dy8	90.2(2)
O5—Dy5—N5	133.4(2)	O22—Dy9—O31	78.6(2)	Dy9—O31—Dy10	89.5(2)
O5—Dy5—N6	125.9(2)	O22—Dy9—O32	144.2(2)	Dy9—O32—Dy12	99.0(2)
O6—Dy5—O4	74.3(2)	O22—Dy9—O33	79.1(2)	Dy9—O33—Dy8	90.9(2)
O6—Dy5—O5	70.3(2)	O22—Dy9—O34	76.5(2)	Dy9—O33—Dy12	100.1(2)
O6—Dy5—N5	69.3(2)	O22—Dy9—O40	94.3(3)	Dy12—O33—Dy8	97.2(2)
O6—Dy5—N6	151.3(2)	O22—Dy9—N19	151.3(2)	Dy8—O34—Dy9	91.8(2)
O8—Dy5—O3	91.1(2)	O26—Dy9—N19	92.9(3)	Dy8—O34—Dy12	99.2(2)
O8—Dy5—O4	74.5(2)	O31—Dy9—O26	68.0(2)	Dy12—O34—Dy9	99.0(3)
O8—Dy5—O5	136.1(2)	O31—Dy9—O32	136.7(2)	Dy8—O35—Dy12	98.9(2)
O8—Dy5—O6	100.7(2)	O31—Dy9—O34	138.5(2)	Dy8—O36—Dy7	89.2(2)